Constitutive activation of Fyn kinase induces dual kinase modulation of the cardiac voltage-gated sodium channel, $Na_v1.5$

by

Mohammed Hassan-Ali

B.A. (Hons.), McMaster University, 2009

THESIS SUBMITTED IN PARTIAL FULFILLMENT
OF THE REQUIREMENTS FOR THE DEGREE OF
MASTER OF SCIENCE

in the
Department of Biomedical Physiology and Kinesiology
Faculty of Science

SIMON FRASER UNIVERSITY

Fall 2011

Approval

Name: **Mohammed Hassan-Ali**

Degree: **Master of Science (Biomedical Physiology and Kinesiology)**

Title of Thesis: ***Constitutive activation of Fyn kinase induces dual kinase modulation of the cardiac voltage-gated sodium channel, $Na_v1.5$***

Examining Committee:

Chair: **Dr. Will Cupples**
Professor, Biomedical Physiology and Kinesiology

Dr. Peter Ruben
Professor, Biomedical Physiology and Kinesiology
Senior Supervisor

Dr. Glen Tibbits
Professor, Biomedical Physiology and Kinesiology
Supervisory Committee Member

Dr. Tom Claydon
Assistant Professor, Biomedical Physiology and Kinesiology
Supervisory Committee Member

Dr. Mark Paetzel
Associate Professor, Molecular Biology and Biochemistry
Simon Fraser University
External Examiner

Date Defended/Approved: November 3, 2011

Declaration of
Partial Copyright Licence

Abstract

Ion channels are critical regulators of excitability in neurons and muscle. The cardiac sodium channel, $Na_v1.5$, is responsible for the initial upstroke of the action potential in ventricular myocytes. Post-translational modifications, such as phosphorylation, modulate $Na_v1.5$. During physiological events, constitutive activation of one or more enzymes results in the integration of signal transduction pathways, thereby altering channel modulation. Specifically, previous studies implicate the integration of PKC and Fyn kinase signal transduction pathways. I studied the effects of dual kinase modulation in $Na_v1.5$ by using Fyn kinase (Fyn) and a partially-selective PKC inhibitor, Bisindolylmaleimide-1 (BIM1). Whole-cell voltage clamp experiments were performed using HEK293 cells co-expressing $Na_v1.5$ and either FynCA (constitutively active) or FynKD (kinase dead, which exerts a dominant-negative effect on tyrosine phosphorylation). Cells co-expressing $Na_v1.5$ + FynCA (without BIM1) showed (i) a significant left shift in the mid-point of steady-state fast inactivation, (ii) accelerated rate of fast inactivation, and (iii) increased non-inactivating sodium current, all of which were not seen in $Na_v1.5$ + FynKD (without BIM1), control or $Na_v1.5$ + FynCA + BIM1 experiments. These results indicate that constitutive activation of Fyn (i) confers dual kinase modulation of $Na_v1.5$ and (ii) leads to the hypoexcitability of cells, which may be pro-arrthythmogenic.

Keywords: Fyn kinase; PKC; sodium channel; phosphorylation

Acknowledgements

My research would be incomplete without acknowledging key members. First and foremost, I would like to thank Dr. Peter Ruben for giving me the opportunity to work and study in his lab. His passion and knowledge for ion channel physiology provided me a strong foundation to grow as a scientific researcher. I am very grateful to have contributed to science and its community.

At the same time, my progress as a student would not be complete without the support and guidance of my supervisory committee members: Dr. Glen Tibbits, Dr. Thomas Claydon, and Dr. Mark Paetzel.

I would also like to acknowledge my lab mates for accepting me into the lab and sharing their wisdom: Dr. Yuriy Vilin, Dr. Stan Sokolov, David Jones, Paul Lee, Csilla Egri, and Colin Peters. Specifically, Dr. Vilin helped me with starting up my project while Colin Peters assisted me with the cardiac action potential modeling.

Finally, I would like to thank my family for their positivity and encouragement.

Table of Contents

List of Figures and Tables

Glossary

Na_v	Voltage-gated sodium channel
Na_vAb	Voltage-gated sodium channel of *A. butzleri*
SCN5A	Gene encoding $Na_v1.5$
I_{Na}	Sodium current
I_{sus}	Sustained macroscopic current
$I_{K(ATP)}$	ATP-sensitive potassium current
I_{Ks}	Slow delayed rectifier potassium current
I_{Kr}	Rapid delayed rectifier potassium current
I_{Kur}	Ultra-rapid delayed rectifier potassium current
I_{to}	Inward transient outward potassium current
I_{CaL}	L-type calcium current
I_h	Pacemaker current
$V_{1/2}$	Midpoint of (in)activation
k	Slope factor
AU	Arbitrary units
SF	Selectivity filter
IFM motif	I = Isoleucine, F = Phenylalanine, M = Methionine
DEKA	D = Aspartic acid, E = Glutamic acid, K = Lysine, A = Alanine
APD	Action potential duration
CAP	Cardiac action potential
LQT3	Long QT syndrome 3
BrS	Brugada Syndrome
LV	Left ventricular dysfunction
HF	Heart failure
SH	Src homology domain
HCN	Hyperpolarization-activated cyclic nucleotide gated channels
NO	Nitric oxide
ROS	Reactive oxygen species
DRG	Dorsal root ganglion neurons
CML	Chronic myelogenous leukemia
IC	Intracellular
EC	Extracellular
HEK293	Human embryonic kidney 293 cells
tsA201	HEK293 cells subclone, stably transfected with SV40 large T-antigen
CHO	Chinese hamster ovary cells
COS7	CV-1 (simian) in Origin, and carrying the SV40 genetic material
RPE	Retinal pigment epithelial cells

EGTA	Ethylene glycol tetraacetic acid
HEPES	(4-(2-hydroxyethyl)-1-piperazineethanesulfonic acid)
DMEM	Dulbecco's modified eagle medium
FBS	Fetal bovine serum
eGFP	Enhanced green fluorescent protein
ANOVA	Analysis of variance
SEM	Standard error of the mean
Q_{10}	Temperature coefficient
IC_{50}	Half maximal (50%) inhibitory concentration
GPCR	G-protein coupled receptor
S/T	Serine/Threonine
Y	Tyrosine
PO^{4-}	Phosphate group
GDP	Guanosine diphosphate
GTP	Guanosine triphosphate
PKA	Protein kinase A
cAMP	Cyclic adenosine monophosphate
PKC	Protein kinase C
PKI	Protein kinase inhibitor
PKCI	Protein kinase C inhibitor
PTK	Protein tyrosine kinase
Src	Sarcoma
CSK	c-Src tyrosine kinase
FynCA	Fyn kinase constitutively active
FynKD	Fyn kinase dead (or catalytically inactive)
CaMKII	Ca^{2+}/calmodulin dependent protein kinase II
EGFR	Epidermal growth factor receptor
FAK	Focal adhesion kinase
Pyk2	Protein tyrosine kinase 2
PP2	Protein phosphatase 2
RPTPβ	Receptor protein tyrosine phosphatase beta
OA	Okadic acid or Oleic acid
OAG	1-oleyl-2-acetyl-*sn*-glycerol
BIM1	2-[1-(3-Dimethylaminopropyl)-1H-indol-3-yl]-3-(1H-indol-3-yl)maleimide hydrochloride or Bisindolylmaleimide-1
AIP	Autocamtide-2 related inhibitory peptide
MS1	2-[1-(3-aminopropyl)indol-3-yl]-3-(indol-3-yl)-N-methylmaleimide

1. Introduction

The voltage-gated sodium channel (Na_v) is responsible for the initial depolarizing phase of the action potential in most excitable cells [1]. The channel is composed of an α-subunit consisting of four domains (DI to DIV) [2]. Each domain comprises six transmembrane alpha helical segments (S1 to S6), with both the N- and C-termini facing the intracellular side [2]. The S5 and S6 segment of each domain is separated by a P-loop region that passes through the channel [3]. The P-loop is an alpha helix-turn beta strand motif in which the selectivity filter (SF) is located [3]. Each segment is approximately 20 to 30 amino acids in length [4]. The S1-S3 and S5-S6 are hydrophobic as they are primarily composed of isoleucine, leucine, valine, and phenylalanine residues [4]. The S4 segment, however, is unique because it has a positively charged residue, an arginine or lysine, at every third position; thus, it is called the voltage sensor because membrane potential changes its conformation [5]. Between S6 of DIII and S1 of DIV, lies a linker region that contains the IFM (isoleucine, phenylalanine, and methionine) motif, which is known as the inactivation gate and is responsible for occluding the pore to prevent the flow of ions [2]. Recently, Payandeh et al., were first to crystallize the voltage-gated sodium channel α-subunit from *A. butzleri* (Na_vAb) [6]. This bacterial crystal structure represents an ancestral form of vertebrate Na_v channels even though both share similar pharmacological and structural features. Figures 1A and B provide the first three-dimensional crystal structure of Na_vAb. In addition, the α-subunit may be associated with up to four β-subunits (β1- β4) [2]. The β-subunits belong to the Ig-like superfamily and are single transmembrane glycoproteins with an intracellular C-terminus and an extracellular N-terminus [7]. β1 and β3 are non-covalently linked to the α-subunit while β2 and β4 are covalently linked via disulphide bond [8]. Only the α subunit, however, is necessary for channel function [9]. The roles of β-subunits are varied and may include: current density, channel kinetics, channel trafficking and membrane anchoring [9, 10]. The SF of the voltage-gated sodium channel consists of one residue per domain (DEKA or aspartic acid, glutamic acid, lysine, and alanine,

respectively) which confers sodium cation selectivity over other monovalent and divalent cations [3]. The structure and function of voltage gated sodium channels are conserved throughout several species [4]. Comparative studies between jellyfish, eel, rat, and mammalian cardiac sodium channels have shown high similarity in the transmembrane segments compared to the intracellular loops, in which there is far less homology [4]. Both the voltage sensor and the inactivation gate are present in all species, as both are essential for channel function [4].

Voltage-gated sodium channels occupy variations of three basic biophysical states: closed, open, or inactivated [11]. At resting membrane potential, the probability that the channel is in the closed conformation is high [12]. Once the membrane is depolarized, current models suggest the S4 segment moves its position relative to the other segments to cause a conformational change [13]. The transition during which the channel goes from the closed state to the open state is called *activation* [11]. At depolarizing membrane potentials, ions pass through the channel and ionic current is generated [11]. During prolonged depolarizations, the inactivation gate acts like a "hinged-lid" and occludes the ion permeation pore [11]. This process is called *fast inactivation* [8]. Wild-type sodium channels can fast inactivate in less than 1 ms and channels must completely repolarize so that another action potential can occur [14]. During fast inactivation, sodium ions cannot pass through the channel [8]. Once repolarized to the resting membrane potential, the channel switches from inactivated state to the closed state [12]. It is important to note that the inactivated state is not the same as closed state [15]. In the inactivated state, the channel is in the open conformation and ions are in the channel but cannot pass through because the conduction pore is blocked from the cytoplasmic side by the "hinged-lid". The closed state conformation does not involve the inactivation gate and the channel is closed in such a way to prevent any ions from accessing the pore both intra- and extracellularly. Because these biophysical states dictate the activity of the channel, post-translational modifications (such as phosphorylation) can modulate channel structure and function.

Figure 1. Three-dimensional structure of Na_vAb.

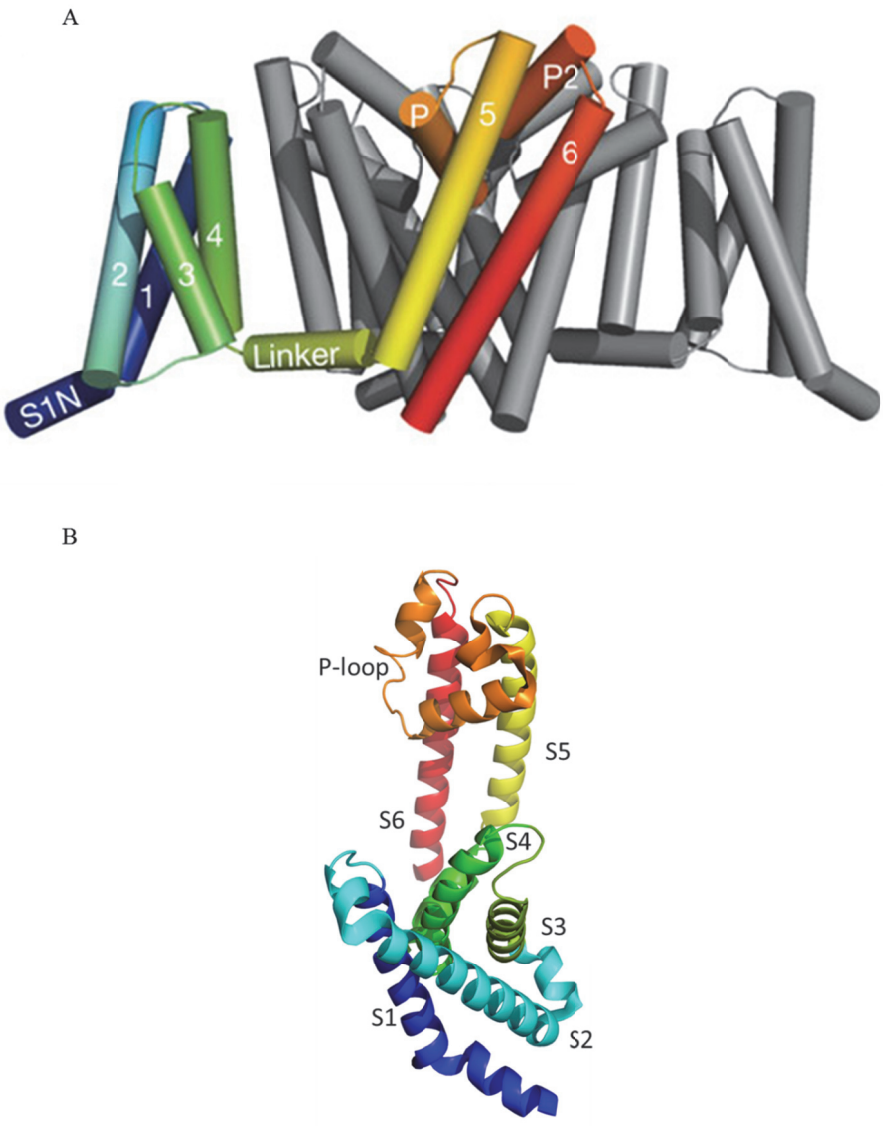

A) The α-subunit of the voltage-gated sodium channel contains four homologous domains (DI – DIV), each comprising six transmembrane segments (S1 – S6). For visual purposes, only one domain is highlighted in color. Both N- and C- termini face the intracellular (IC) compartment. The P-loop region of S5-S6 is partially extracellular (EC) and enters the plasma membrane. B) Topographical view of a single Na_vAb domain. The colours correspond to the transmembrane segments as identified in A) [6].

1.1. Na_v Phosphorylation

1.1.1. Protein Kinase A (PKA)

The 'cardiac' voltage-gated sodium channel, $Na_v1.5$, is responsible for the initial upstroke of the cardiac ventricular action potential [16, 17]. Phosphorylation regulates channel function by the addition of bulky and negatively-charged phosphate groups [18, 19]. Serine, threonine, or tyrosine target residues are located in the cytosolic linker regions of $Na_v1.5$ [20, 21]. cAMP-dependent Protein kinase A (PKA), is a serine/threonine (S/T) kinase comprising two regulatory subunits and two catalytic subunits [19]. An increase in cAMP levels in mammalian cells via G-protein coupled receptor (GPCR) activation causes the two types of subunits to dissociate. The catalytic subunit then phosphorylates target proteins [19]. The target sequence for PKA phosphorylation is -R(R/K)X(S/T)- (X being any amino acid) [19]. The DI and DII linker of rat $Na_v1.5$ contain five of these potential PKA sites [22]. In 1992, Matsuda et al., showed PKA stimulation increased I_{Na} amplitude [22]. Whole-cell patch clamp and single channel inside-out recording on rabbit cardiac myocytes, showed PKA stimulation by isoproterenol and/or forskolin at 25°C. Extracellular bath containing isoproterenol increased I_{Na} amplitude at a test potential of -35 mV (with a holding potential of -90 mV) and increased the rate of inactivation. Forskolin, which raises cytosolic cAMP levels, showed the same effect as isoproterenol. Experiments performed at 15°C showed no significant change, suggesting PKA is temperature dependent. Neither drug affected steady-state activation/inactivation kinetics at either temperature. In two other experiments, (i) the catalytic subunit of PKA alone or (ii) several variations of $G_{s\alpha}$, showed results consistent with those of isoproterenol and forskolin. Using inhibitors to block the effect of PKA showed current reduction beyond control, suggesting constitutive phosphorylation of $Na_v1.5$. All experiments showed enhanced entry into the inactivated state, especially at hyperpolarized potentials. This observation is reportedly due to the addition of phosphate groups by PKA thereby changing the conformation of the channel to become more accessible (for further regulation) and stable [22].

$Na_v1.5$ channelopathies, such as Long QT syndrome (LQT3), are modulated by phosphorylation [23]. At depolarized potentials, wild-type $Na_v1.5$ fully inactivates, whereas mutant channels fail to inactivate [23]. This leads to persistent current (also

known as sustained macroscopic current, I_{sus}), which is potentially arrhythmogenic. In 2003, Tateyama et al., studied the effects of PKA phosphorylation in mutant $Na_v1.5$ channels [23]. PKA activation further enhances I_{sus} in D1790G mutation. The D1790G mutation is located in the C-terminus tail of the channel and the removal of the negative charge (due to the mutation) is essential for PKA modulation. Whole-cell and single channel patch clamp recording, showed cAMP or okadiac acid (OA – a non-specific protein phosphatase inhibitor) application activated PKA. PKA phosphorylation of residues S36 and S525 in $Na_v1.5$ destabilized the inactivated state, causing an increase in I_{sus}. Application of protein kinase inhibitor (PKI) reversed the effects. Changing the polarity of the charge (D1790K), does not generate I_{sus}, but modulation by PKA (and inhibition by PKI) still occurs. D1790E mutation, which maintains the negative charge, does not exhibit I_{sus} or modulation by PKA. In addition, a significant reduction in PKA regulation of D1790G occurs with S36A and S525A mutations suggesting a concerted effect by both the mutation and target S/T residues in the channel for the observed phenotype.

1.1.2. Protein Kinase C (PKC)

The Protein kinase C (PKC) superfamily comprises 12 distinct genes encoding S/T kinases [24, 25]. Unlike PKA, PKC does not have a target sequence for binding [19]. Despite a large family, the isozymes exhibit redundancy in their structure, all of which contain a V5, a kinase, and C1 and C2 domains [24]. PKC regulates $Na_v1.5$ by decreasing I_{Na} amplitude [26]. In 1994, Qu et al., studied PKC activation in rat $Na_v1.5$ expressed in Chinese hamster lung 1610 cells [26]. 1-oleyl-2-acetyl-*sn*-glycerol (OAG) activates PKC. The decrease in I_{Na} amplitude was reported to be partially due to a hyperpolarizing shift in the voltage-dependence of steady-state inactivation; in contrast, steady-state activation remained unchanged. Application of either PKI or protein kinase C inhibitor (PKCI) abolished the effects of OAG. A subsequent study by the same authors showed that the effect of PKC is contingent upon the phosphorylation of the S1505 residue [27]. Using similar conditions to their previous experiment, a S1505A mutation showed a significant reduction in the activation of PKC and no hyperpolarizing shift in steady-state inactivation. It is speculated that the addition of the negative charge on S1505 residue changes the conformation of the channel to stabilize the inactivated state.

An analogous version of this key residue in mice $Na_v1.5$ (S1503) regulates I_{sus} [28]. The activation of PKC via OAG decreases I_{sus}. This effect is greater in LQT mutant channels (Y1795C, 1795H, ΔKPQ). Staurosporine (a non-specific protein kinase inhibitor) or a S1503A mutation removes the decrease in I_{sus}, while a S1503D mutation mimics OAG. Although PKC cannot phosphorylate the S1503D residue, the negative charge of the aspartic acid further reinforces the role of charge in the cytosolic space for the stabilization of the inactivated state.

1.1.3. Fyn Kinase

Non-receptor tyrosine phosphorylation by Src-family kinases regulates $Na_v1.5$ [29, 30]. The Src-family contains nine members with different functions yet structural redundancies [31]. All members contain a SH4, SH3, SH2, and a kinase domain [21]. The SH4 domain, located at the N-terminus, contains (i) Met-Gly-Cys motif and (ii) myristoyl and palmitoyl groups, which anchors the kinase to the lipid membrane for support. Src-family kinases do not have a direct target sequence for tyrosine binding; rather, the SH3 domain binds to -PXXP- motifs in the target protein to phosphorylate any tyrosine residues either upstream or downstream from this motif [19, 21]. Finally, the SH2 domain binds to tyrosine residues on the target protein [21]. One Src-family member in particular, Fyn kinase (Fyn) has been shown to interact with Na_v [21, 29, 30]. The Y531 residue of Fyn is responsible for the catalytic activity of this enzyme [32]. The phosphorylation of this residue by C-src tyrosine (CSK) kinase inhibits Fyn kinase activity. Only by cleaving or dephosphorylating this residue, can Fyn kinase phosphorylate its target protein [32]. The function of Fyn kinase is associated with T-cell development and activation, myelination of neurons, and CNS disorders [33]. In cardiac myocytes, Fyn is activated (via integrin receptors) in response to biomechanical stress leading to the development of cardiac hypertrophy [34]. In 2007, Beacham et al., studied neuronal $Na_v1.2$ phosphorylation by Fyn [21]. The SH3 domain of Fyn binds to the SH3 domain of $Na_v1.2$ (located in the linker region between DI and DII). Mutational analysis showed that removal of the SH3 domain of $Na_v1.2$ prevents Fyn binding and modulation. The SH3 domain of Fyn phosphorylates Y66 and Y1893 residues in $Na_v1.2$. The additional phosphorylation induces the binding of the SH2 domain of Fyn to $Na_v1.2$. Co-expression of Fyn and $Na_v1.2$ in tsA201 cells revealed no change in the voltage-

dependence of activation compared to $Na_v1.2$ alone. There was, however, a significant -5.9 mV shift in the voltage-dependence of inactivation.

In 2005, Ahern et al. studied Fyn regulation of $Na_v1.5$ using HEK293 cells [29]. Since HEK293 cells have endogenous Fyn activity, basal phosphorylation of $Na_v1.5$ is present. Application of insulin further activates Fyn phosphorylation. Activation by insulin, does not affect steady-state activation, but there was a significant depolarizing shift in steady-state inactivation curve, suggesting a destabilization of the fast-inactivated state. Co-expression of either a constitutively active Fyn (FynCA) or a kinase-dead Fyn (FynKD) showed further modulation by Fyn. The FynCA mutant lacks the inhibitory carboxyl terminus (deletion of residues 525 to 537), whereas the FynKD mutant has a point mutation at K299M that renders the enzyme catalytically inactive. The endogenous activity of Fyn increases in the presence of FynCA and decreases in the presence of FynKD. In Ahern's experiments, $Na_v1.5$ co-expressed with FynCA showed an +11 mV depolarizing shift in steady-state inactivation and an increase in the rate of recovery from fast inactivation. The depolarizing shift in steady-state inactivation increased the window current, which enhances excitability near the resting membrane potential. The increase in intracellular negative charge by FynCA leads to the destabilization of the fast-inactivated state, which is inconsistent with PKC experiments and the results obtained from Fyn expression in $Na_v1.2$ [26, 27, 35]. $Na_v1.5$ co-expressed with FynKD showed a hyperpolarizing shift in steady-state inactivation, greater than control, suggesting the kinase-dead mutant competes with, and displaces, endogenous Fyn from potential binding sites on the channel, thereby exerting a dominant-negative effect. Ahern's experiments, however, assume that only one kinase modulates the channel at a time (as a PKC inhibitor, BIM1, was used in all experiments) and that signal transduction pathways are isolated from one another. Physiologically, channel phosphorylation is a dynamic process and involves multiple kinases and numerous pathways, and this complexity warrants further investigation.

2. Purpose

The above Introduction separates PKA, PKC, and Fyn kinase into three distinct classes, each having separate pathways. Although each class of kinase differentially affects $Na_v1.5$, there is cross-talk between the kinases [36-38]. Activation or deactivation of enzymes can occur either upstream or downstream during a signaling cascade [38]. Studies have shown that the constitutive activation of a kinase can lead to changes in various signal transduction pathways [39]. Two kinases in particular, PKC and Fyn kinase, when activated share a signal transduction pathway during numerous events including: ischemia/reperfusion, cancer therapy, and retinal development (Fig. 2) [38-40]. Therefore, investigating dual kinase modulation on voltage-gated ion channels may provide additional modulatory mechanisms during physiological events.

Figure 2. $Na_v1.5$ modulation by phosphorylation.

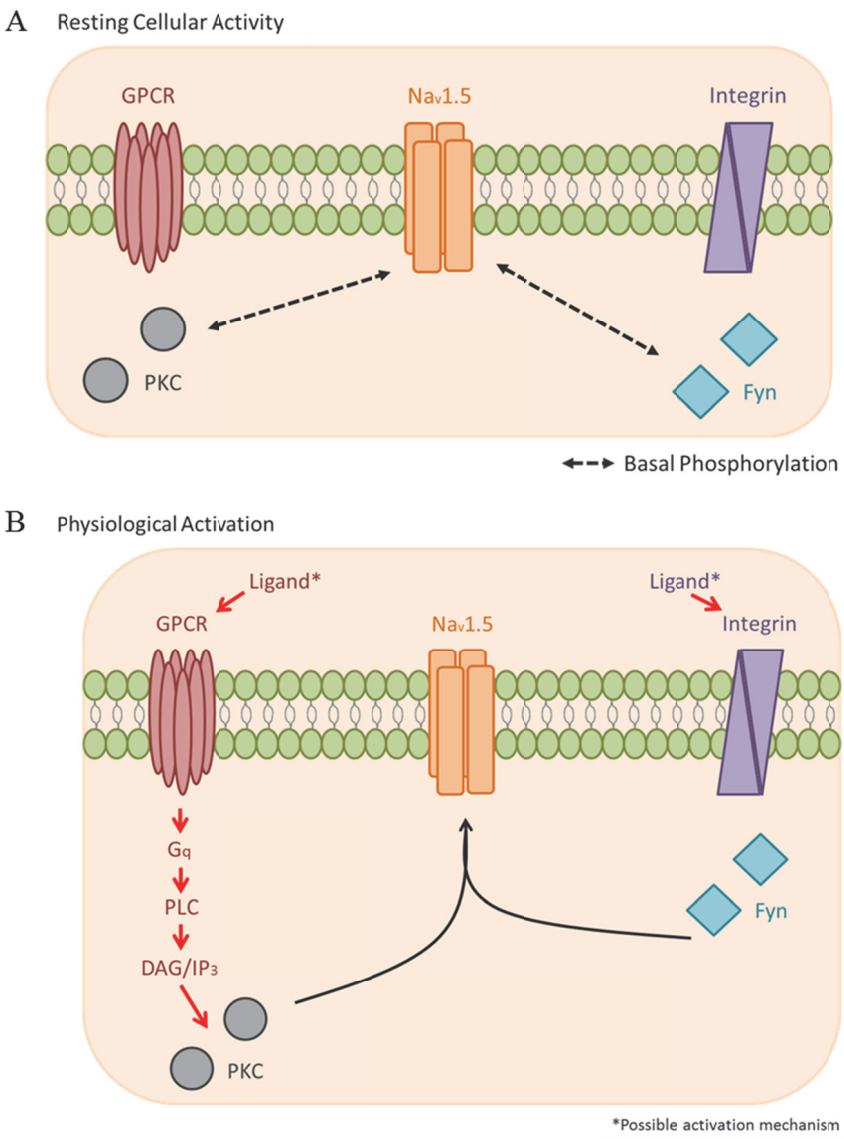

A) Basal phosphorylation of $Na_v1.5$ via two independent pathways. Without GPCR stimulation, PKC isozymes may modulate $Na_v1.5$ at resting levels by phosphorylating intracellular serine/threonine residues. Without integrin activation, Fyn kinase may modulate $Na_v1.5$ at resting levels by phosphorylating intracellular tyrosine residues. Here, the rate of phosphorylation and dephosphorylation is at equilibrium. B) Events such as stress or growth leads to the activation of one or more kinases. Extracellular ligands may bind to (i) GPCRs leading to the activation of PKC via signaling cascade or (ii) integrins leading to the constitutive activation of Fyn kinase. Here, the equilibrium shifts towards phosphorylation. Activation of one or more kinases is thought to lead to a shared pathway, leading to dual kinase modulation of target channel.

3. Hypothesis

The biophysical properties of post-translational modification of $Na_v1.5$ were studied. The experiments, therefore, consisted of $Na_v1.5$, PKC, and Fyn kinase as well as a Bisindolylmaleimide-1 (BIM1, a partially selective PKC inhibitor). Dual kinase modulation is observed when one of the kinases is constitutively activated. If there are significant changes in $Na_v1.5$ kinetics, then the study has provided evidence that $Na_v1.5$ (i) is differentially modulated by two kinases and (ii) is possibly involved in cardiac (dys)function.

The specific aims of this study were:

1. testing the hypothesis that $Na_v1.5$ co-expression, with a constitutively active form of Fyn, stabilizes the fast inactivated state;
2. testing the hypothesis that $Na_v1.5$ co-expression, with a kinase dead form of Fyn, destabilizes the fast inactivated state;
3. testing the hypothesis that PKC inhibition alters Fyn kinase regulation in $Na_v1.5$ to determine whether there is dual kinase modulation of Na_v.

Finally, I sought to use the results of these tests to speculate on the physiological relevance of dual kinase modulation.

4. Materials and Methods

4.1. Fyn kinase sequencing

Two Fyn mutants in pCS2+ vector were used: (i) constitutively active Fyn (FynCA), and (ii) kinase-dead Fyn (FynKD). Both Fyn kinase constructs were generously provided by Todd Holmes and Al Llamas (University of California, Irvine, CA). Sequencing of the mutants was performed by Eurofins MWG Operon (Huntsville, AL). Restriction enzymes to cut sequence included ApoI and SmaI (WebCutter 2.0, New Haven, CT). Sequence alignment to confirm both constructs and their respective mutations was performed using LALIGN (Lausanne, SZ).

4.2. DNA clones, Transfection, and Cell Culture

Wild-type $Na_v1.5$ (α subunit) was cloned into pRC-CMV vector (A.L. George, Vanderbilt University, Nashville, TN). A heterologous expression system using HEK293 cells were cultured using media comprising DMEM 1X (Gibco), FBS 20% (Gibco) and 10000 U penicillin/streptomycin solution (Sigma). Cells were then transiently transfected (Polyfect, Qiagen) with enhanced Green Fluorescent Protein, eGFP (pEGFP vector was provided by Brett Adams, Utah State University, Logan, UT) to identify channel and enzyme expression.

4.3. PKC Inhibition

HEK293 cells endogenously express 6 PKC isozymes in significant levels: α, ε, ζ, η, θ, ι [41]. Many PKC inhibitors can block one or more of the isozymes listed above. Selecting the appropriate drug can be difficult as the IC_{50} of certain PKC isozymes overlap with other protein kinases outside of the PKC family [42]. The hydrochloride

variant (or water soluble form) of BIM1, can effectively block α, ε, ζ in nanomolar concentrations without blocking PKA (which requires micromolar concentrations). Due to the ubiquitous role of PKC in signal transduction pathways, blocking all 6 isozymes is unnecessary; certain isozymes have opposing roles and complete block may produce adverse effects [43].

Thus, 2-[1-(3-Dimethylaminopropyl)-1H-indol-3-yl]-3-(1H-indol-3-yl)maleimide hydrochloride (Bisindolylmaleimide-1 or BIM1) was used for these experiments (Cedarlane, Burlington, ON). A concentration of 135 nM was dissolved into the extracellular solution. A total of six sets of experiments were conducted (Fig. 3).

Figure 3. Expected mechanisms of activation/block of $Na_v1.5$.

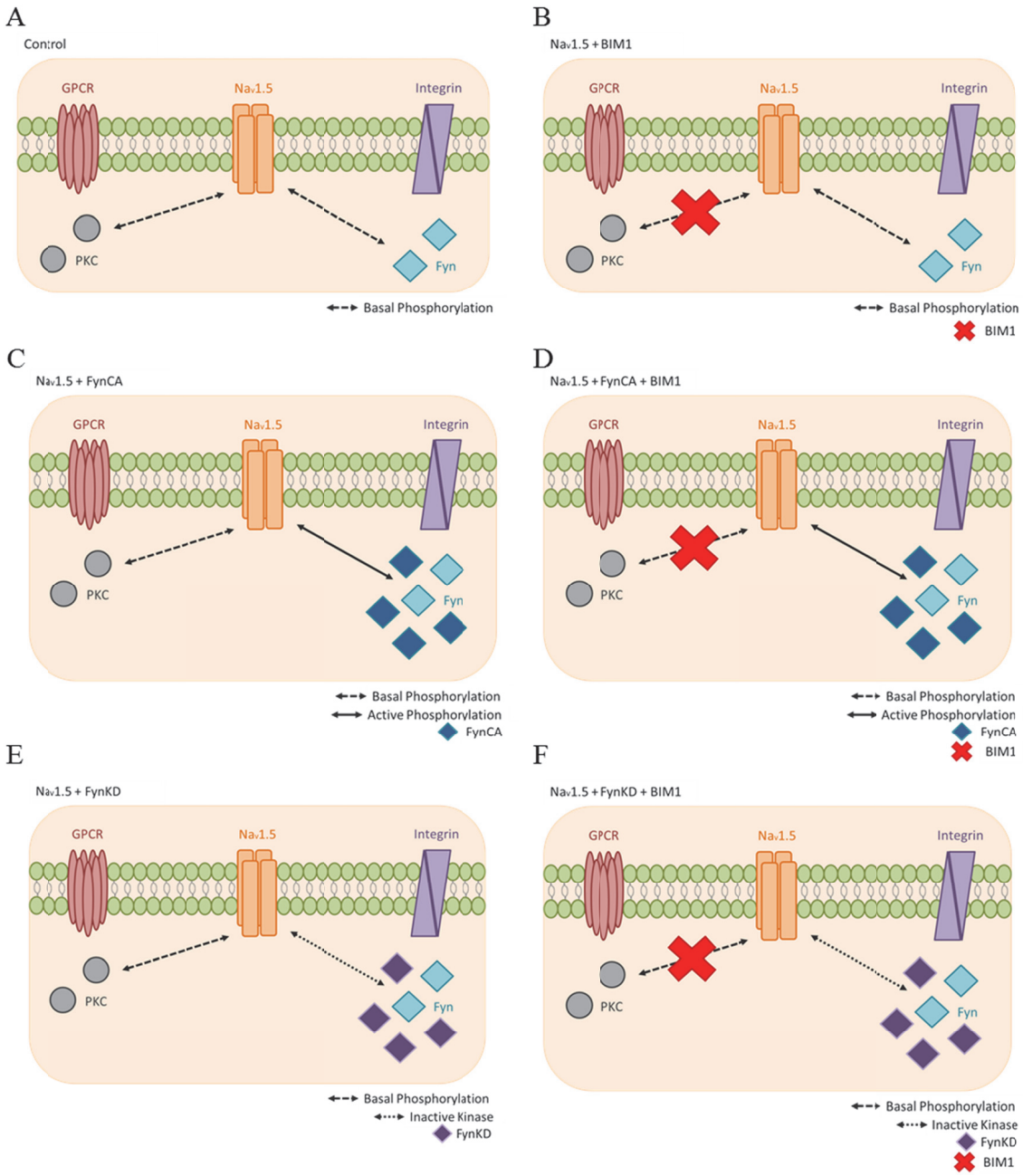

The experiments were divided into two groups: Without BIM1 and With BIM1 (as indicated by a red X). Without BIM1 group comprised three treatments: A) control – measurements recorded with $Na_v1.5$ being expressed only, C) $Na_v1.5$ + FynCA, the channel is co-expressed with a constitutively active Fyn kinase (dominant positive) and E) $Na_v1.5$ + FynKD, where the channel is co-expressed with a kinase dead mutant (dominant negative). The same treatments are repeated in the With BIM1 group with the addition of the PKC inhibitor: B) $Na_v1.5$ + BIM1, D) $Na_v1.5$ + FynCA + BIM1, and F) $Na_v1.5$ + FynKD + BIM1.

4.4. Electrophysiology

Ionic currents were measured using the whole-cell patch clamp technique. Pipettes were made from borosilicate glass (Sutter Instruments, Novato, CA) with dimensions of 10 cm length, outer diameter of 1.5 mm, and inner diameter of 1.10 mm, and fabricated using a P-1000 pipette puller (Sutter Instruments, Novato, CA). Borosilicate glass provided higher resistance pipettes as well as low dielectric loss and noise reduction [44]. Once pulled, pipette tips, were dipped in dental wax (Patterson, Richmond, BC) before being fire-polished using a pipette microforge MF-830 (Narishige Japan). The wax reduced the pipette-bath capacitance and background noise [44, 45]. The resistance of the pipette ranged from 1-1.3 MΩ. Only cells with a seal resistance of 1 GΩ or greater were used. Although series resistance compensation results in better voltage control, compensation can increase the time constant by slowing down the charging of the cell membrane capacitance (because it impedes the flow of the capacitive charging currents when a voltage step is applied to the pipette electrode). Adequate voltage control was achievable by using low-resistance pipettes. Thus, series resistance compensation was not used during recordings and data analyses were performed with recordings which had series resistance less than 3.5 MΩ.

The pipette solution contained (in mM): 130 CsCl, 10 NaCl, 10 EGTA, and 10 HEPES adjusted to pH 7.4 with CsOH. The extracellular bath contained (in mM): 140 NaCl, 4 KCl, 2 $CaCl_2$, 1 $MgCl_2$, and 10 HEPES adjusted to pH 7.4 with CsOH.

Cells were visualized using a Nikon Diaphot inverted microscope (Nikon, Mississauga, ON). A micromanipulator MP-225 (Sutter Instruments) was used to position the patch pipette. Data were collected using an EPC9 Patch Clamp Amplifier (HEKA, Lambrecht, Germany), 2 to 5 minutes after whole-cell configuration was achieved. Sample frequency was set to 50 kHz (20 μs) and filter frequency was 10 kHz to capture the fast kinetics of Nav1.5 [46]. All measurements were conducted at room temperature (22°C).

4.5. Action Potential Modeling

An action potential model was used to understand how the results from these experiments may affect the sodium contribution to a cardiac action potential (CAP) in a cardiomyocyte. The original ten Tusscher CAP model was programmed into Python code using the modules NumPy (Enthought Inc., Austin, TX), and then updated with recent calcium current and slow delayed potassium current equations [47-49]. Late persistent I_{Na} was added using the formulas of Hund and Rudy [50]. To better reflect the experimental data, maximal sodium conductance value was replaced using the Luo-Rudy dynamic model and the late sodium maximal conductance value was changed to reflect the data collected by Zygmunt et al. [51, 52]. Slow delayed rectifier potassium conductance (G_{Ks}) was also altered to incorporate the role of internal calcium concentrations on G_{Ks} [53]. Together, the data show differing persistent I_{Na} in different layers of the ventricular myocardium. To reflect the different sodium current properties under different phosphorylation conditions, steady-state conductance, inactivation and fast inactivation time constants (for both recovery and onset) values were incorporated into the model. Data were Q_{10} adjusted using the same methods as ten Tusscher et al. and Nagatomo et al. [47, 54]. The action potential model was run for midmyocardial ventricular cardiomyocytes at 1 Hz for 50 action potentials.

4.6. Data Analysis and Statistics

Data were recorded using Patch Master (HEKA) on an iMac computer (Apple, Cupertino, CA). Data were analyzed using Fit Master (HEKA) and Igor Pro (Wavemetrics, Portland, OR). G-V relations were fitted to the Boltzmann Equation:

$$G(V) = \frac{1}{1+\exp[-qF\ (V-V_{mid})/RT]} \qquad (1)$$

where G(V) is conductance, q is ion charge, F is Faraday's constant (9.6485×10^4 C mol^{-1}), V is the test pulse membrane potential, V_{mid} is the activation midpoint of the

voltage corresponding to 50% of the maximal conductance, R is the gas constant (8.3145 V C mol^{-1} K^{-1}) and T for absolute temperature in degrees Kelvin (295.15 K).

Recovery and onset of fast inactivation data were fitted by a single exponential fit using:

$$y = y_o + A\exp\left[-(x-x_o)/\tau\right] \qquad (2)$$

where y is peak amplitude at test pulse, y_o is asymptote value, A is current amplitude, x is the time at which recording is being taken, x_o is 0, and τ is the time constant.

A P/4 method was used for leak subtraction. Leak delay, size, and holding voltage is set as 20.0 ms, 0.250 (before test pulse), and -100 mV, respectively.

Using SPSS 19 (IBM, Armonk, NY) statistical comparisons were made using two-way ANOVA with Tukey's post-hoc test to determine which appropriate levels were significantly different from each other. Conductance and steady-state fast inactivation midpoint and slope statistical analyses were as follows:

1. Control ($Na_v1.5$ alone)
2. ENZYME (2 levels) – FynCA, FynKD
3. DRUG (2 levels) – With BIM1, Without BIM1

Voltage dependence of fast inactivation and open-state fast inactivation also included:

4. Control ($Na_v1.5$ alone)
5. ENZYME (5 levels) – $Na_v1.5$ + BIM1, $Na_v1.5$ + FynCA, $Na_v1.5$ + FynCA + BIM1, $Na_v1.5$ + FynKD, and $Na_v1.5$ + FynKD + BIM1
6. mV (11 levels for voltage dependence ranging from -130 mV to -30 mV; 7 levels for Open-state ranging from -50 mV to +10 mV)

Results are presented as means ± SEM unless otherwise stated. Statistical significance is assumed to be $P<0.05$.

4.7. Study Limitations

4.7.1. Cell Preparation and Recordings

Limitations to this study range from experimental design to data interpretation. Although heterologous expression systems provide a convenient vehicle with which to perform electrophysiological experiments, the probability of cells co-expressing three proteins can be difficult. The Polyfect agent weakens the plasma membrane, which causes difficulty in successful patching and recording. Even with the eGFP marker, there were cells without current after whole-cell mode was achieved. Cell growth occurred at 37° C whereas recordings were conducted at 22°C. Enzymes and other proteins have optimal activity at certain temperatures which may affect the significance and the relevance of results. The use of CsCl, which is more appropriate for experiments dealing with phosphorylation results in less electrically stable seals. Therefore, for certain analyses such as window current, matched pairs were difficult to achieve due to (i) the short-time frame of recording and (ii) the drug application breaking the seal.

4.7.2. Cesium Chloride versus Cesium Fluoride in the Pipette (Intracellular) Solution

I used cesium chloride in the pipette (intracellular) solution instead of the CsF used in previous studies of Fyn kinase and sodium channels [29]. Although CsF provides longer lasting and electrically stable seals, the high electronegativity of the fluoride ion is problematic when studying signal transduction pathways. Coste et al., studied $Na_v1.8$ and $Na_v1.9$ (both found in dorsal root ganglion (DRG) neurons) and found that the use of fluoride in pipette solution caused hyperpolarizing shifts in voltage-dependence of activation and inactivation for Nav1.9 [55]. In 1999, Vargas et al., studied I_h (HCN channels) current and found fluoride in the pipette solution caused a significant hyperpolarizing shift in steady-state activation and altered PKA activity [56]. Vargas further confirmed their results by using perforated-patch clamp recordings. The fluoride ion is small enough to pass through the nystatin generated pores. Finally, fluoride use in cardiac L-type calcium channels increased channel activity affecting G-protein interactions [57].

Fluoride can form complexes with aluminum, generating AlF^{4-} – a potent activator of G-proteins [58]. The chemical structure of AlF^{4-} is similar to the phosphate (PO^{4-}) group enabling the former to interact with GDP near the α-subunit of G-proteins which mimics the function of GTP thereby initiating a signaling cascade [59]. Although aluminum is found in cells in trace amounts, AlF^{4-} is formed from (i) using equipment when creating solutions, or (ii) the contamination of solution(s) when operating machinery [59, 60].

Fluoride is also a known inhibitor of serine/threonine phosphatases and is usually added in extracellular buffers to prevent dephosphorylation [29, 59]. In 2009, the updated whole-cell voltage clamp protocols by Cummins et al. suggested that fluoride should only be used when cells are pre-treated with the desired activator/inhibitor so that the effect of the activator/inhibitor is determined by comparing treated versus non-treated cells [61]. This suggestion, however, was presented with a caveat. The activation of signal transduction pathways on channels occurs in real-time; from the time that the kinase activator/inhibitor is co-expressed (or applied); it is already modulating the target protein even before the experiment starts. Therefore, Cummins et al, strongly suggested to avoid the use of fluoride as it will affect the modulation of channels [61]. Consequently, using CsCl in pipette solutions avoids these issues and is therefore more appropriate and relevant for my study [55, 61]

4.7.3. β-Subunit Modulation

The β-subunits of $Na_v1.5$ have been implicated in numerous functions such as channel trafficking and anchoring the channel to the plasma membrane [10]. The cytosolic portion of β1 subunit has been studied and can be tyrosine dephosphorylated by Receptor Protein Tryosine Phosphtase β (RPTPβ) [1, 10]. Tyrosine phosphorylated β1-subunits in cardiac myocytes were localized to intercalated disks whereas non-phosphorylated β1-subunits were found in T-tubules [62]. Although the α-subunit is only needed for the voltage properties of $Na_v1.5$, it is possible that co-expression with β subunit could affect the number of ion channels expressed in the plasma membrane which can contribute to the amount of sodium current [10]. Ko et al., co-expressed β1 and β3 (individually or combined) with $Na_v1.5$ in Chinese Hamster Ovary (CHO) cells and discovered significant hyperpolarizing shifts in steady-state inactivation [63]. Co-

expression of β-subunit also resulted in reduced late I_{Na} and slowed recovery from inactivation. HEK293 cells endogenously express a β1 splice variant which has shown to modulate α-subunit inactivation [64]. Therefore, it may be difficult from these experiments to quantify whether the β-subunit is actively modulating the α-subunit and if there are significant changes in $Na_v1.5$ kinetics and voltage dependence.

4.7.4. Channel modulation due to binding or phosphorylation?

Electrophysiological experiments in the absence of molecular biology techniques may lead to misinterpretation of results. For instance, it is plausible that a kinase may indirectly modulate the channel by simply binding to the channel rather than directly phosphorylating the channel. In 2007, a study by Jiang et al., studied CaMKII modulation of $Ca_v2.1$ channels [65]. Ca^{2+}/calmodulin-dependent protein kinase II (CaMKII) is another serine/threonine kinase that modulates voltage-gated ion channels (including $Na_v1.5$) [65-67]. CaMKII is autoinhibited under basal conditions and activates only in response to Ca^{2+} signals. Whole-cell recordings in tsA201 cells revealed that CaMKII slows inactivation by shifting the voltage dependence in the positive direction. To inhibit the catalytic domain of CaMKII, Autocamtide-2 related inhibitory peptide (AIP) was used. AIP did not change the kinetics or voltage dependence of $Ca_v2.1$ channels. To confirm this result, immunocytochemistry was performed using CaMKII with a phosphospecific antibody. AIP reduced CaMKII autophosphorylation without altering $Ca_v2.1$ modulation. It is therefore possible that similar issues could be present in this study. Rather than channel modulation via phosphorylation, it may be enzyme binding that changes the kinetics and voltage dependence of the channel. Future studies using molecular biology techniques and appropriate antibodies would confirm phosphorylation of $Na_v1.5$. A Western blot with antiphosphotyrosine antibody could be used to detect differences in tyrosine phosphorylation when FynCA or FynKD is co-expressed.

4.7.5. Action Potential Modeling

To elucidate the physiological relevance of post-translational modifications on $Na_v1.5$, inputting data into an action potential model can be performed. An appropriate model can therefore make predictions on the effect of a single ion channel with respect to rest of the cardiac myocyte. It is important to note that modeling does not take into

account the post-translational modification of other ion channels. Fyn kinase modulates several ion channels such as: $I_{K(ATP)}$, I_{Ks}, I_{Kr}, I_{Kur} [68-70]. PKC modulates other ion channels such as: I_{Ks}, I_{to}, I_{CaL} [14, 71, 72]. In addition, the model used here represents the cardiac action potential during steady-state and not during cardiac events where there would be constitutive activation of one or more enzymes. Thus, this model provides only a snap-shot of otherwise a complex and dynamic physiological process.

5. Results

5.1. Sodium Current

To ensure that the fluorescing HEK293 cells were expressing $Na_v1.5$, I first measured transient I_{Na}. Current traces (and cells) in which voltage control was not adequate (i.e. due to space clamp, seal breaking, run up/down, changes in series resistance, or no channel expression) were discarded. The current traces (Fig. 4) show graded and sequential steps for each voltage protocol. In cells exhibiting space clamp artefacts, the current trace would indicate a large jump from one voltage to the next. In addition, steady-state fast inactivation curves would shift in the hyperpolarizing direction. Data collected from cells in which the seal ruptured (after whole-cell mode and a period of time) was only used in this study if the recordings were stable up to the point of rupture. For this to occur 0 trains were measured before and after each voltage protocol to ensure that run-up or run-down did not occur. Cells were held at -130 mV and then depolarized to 0 mV for 19 ms and then hyperpolarized to -130 mV for 1 ms for 5 sweeps to view if the cells were stable before and after I ran each voltage protocol.

Figure 4 depicts current traces elicited from a holding potential of -130 mV and depolarized to a range of voltages from -80 to +60 mV in 10 mV steps for a duration of 20 ms. The holding potential ensures that all channels are recovered from fast and slow inactivation (and therefore available for activation) before a voltage protocol was applied.

Figure 4. Sodium current traces.

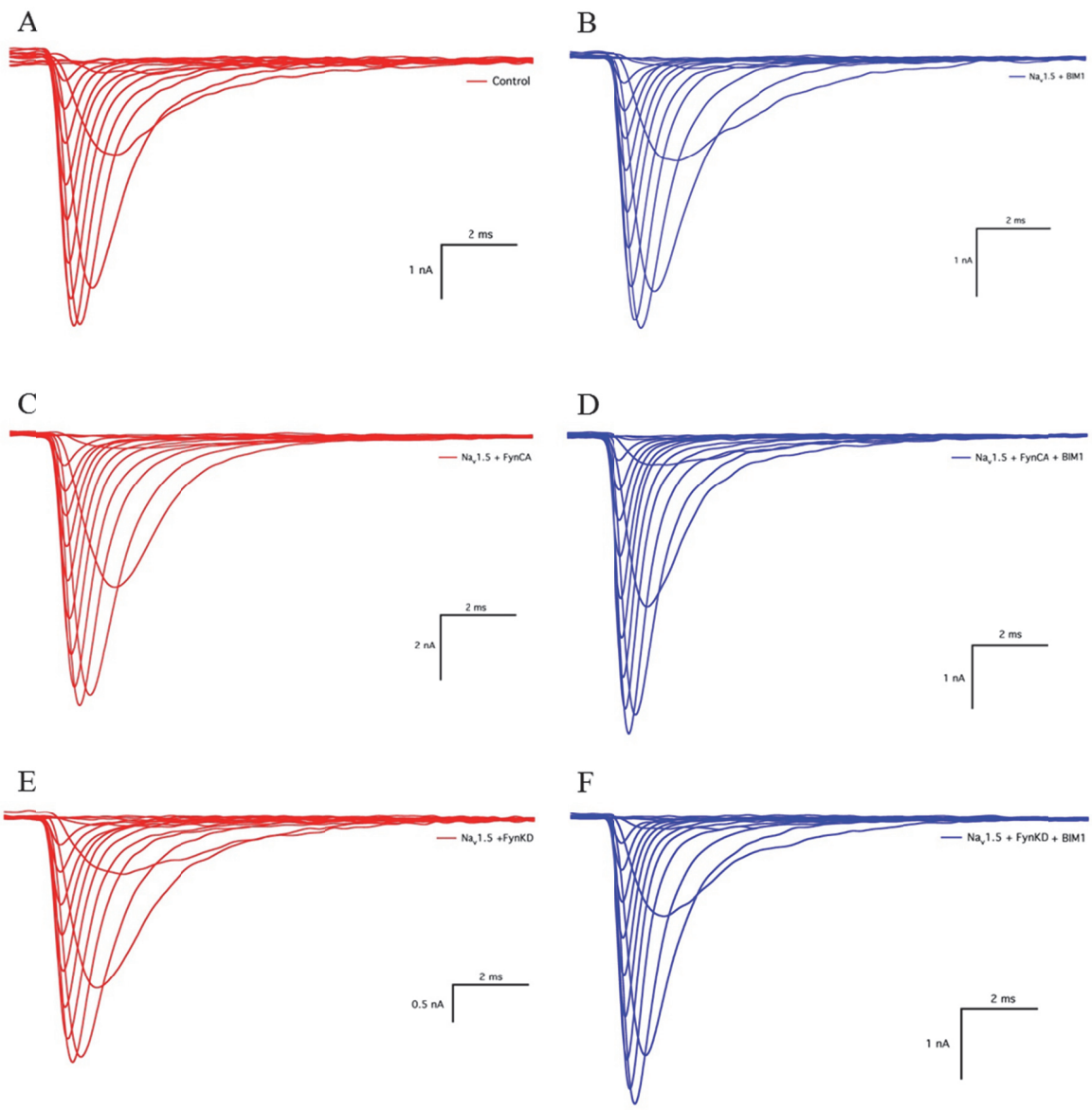

Representative current traces of the six experiments divided into two categories for clarification and comparison: (i) Without BIM1 (red) – which include A) control, C) $Na_v1.5$ + FynCA and E) $Na_v1.5$ + FynKD and (ii) With BIM1 (blue) – which include B) $Na_v1.5$ + BIM1, (D) $Na_v1.5$ + FynCA + BIM1, and (F) $Na_v1.5$ + FynKD + BIM1.

5.1.1. Activation

From the peak of each current trace (Fig. 4), I measured the voltage-dependence of channel activation, by plotting the normalized macroscopic conductance as a function of membrane potential. Conductance was calculated from peak I_{Na} using:

$$G_{Na} = I_{Na}/V\text{-}E_{Na} \quad (3)$$

where G_{Na} is sodium channel conductance, I_{Na} is peak sodium current in response to V (test pulse membrane potential), and E_{Na} is the Nernst equilibrium potential. Conductance curves were fitted with Boltzmann equation (1). Figure 5 shows the mean $V_{1/2}$ of $Na_v1.5$ + FynKD which produced a significant -3.3 mV hyperpolarizing shift compared to $Na_v1.5$ + FynCA. The mean slope of control was steeper than $Na_v1.5$ + FynCA (6.4 and 3.2 respectively). Also, the mean slope of $Na_v1.5$ + FynKD was steeper than $Na_v1.5$ + FynCA (5.4 and 3.2 respectively).

Figure 5. Voltage-dependence of activation.

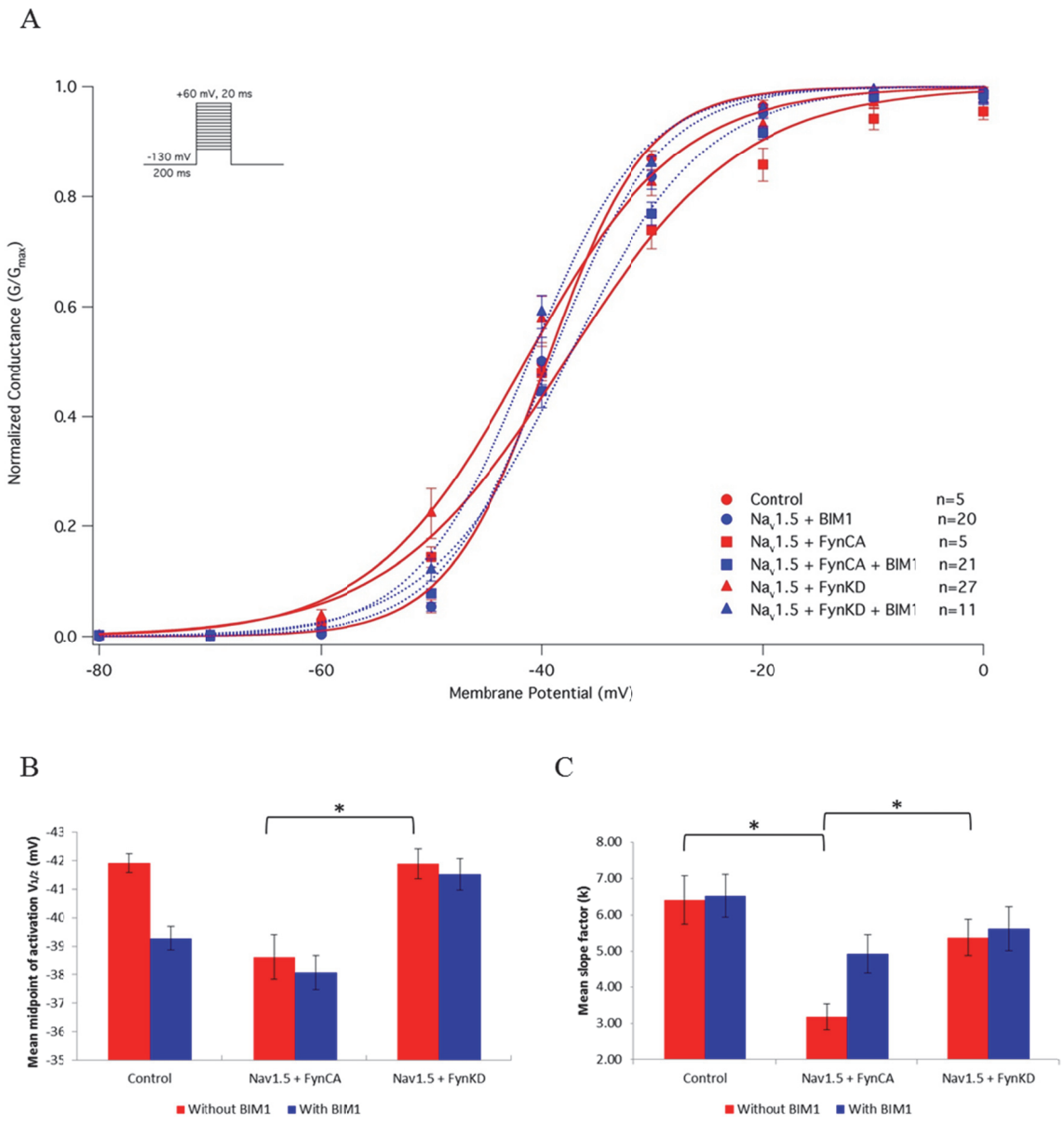

D

	Mean midpoint of activation $V_{1/2}$ (mV)	±SEM	Mean slope factor (k)	±SEM
Control	-41.9	0.3	6.4 [b]	0.7
$Na_v1.5$ + BIM1	-39.3	0.4	6.5	0.6
$Na_v1.5$ + FynCA	-38.6 [a]	0.8	3.2 [bc]	0.4
$Na_v1.5$ + FynCA + BIM1	-38.1	0.6	4.9	0.5
$Na_v1.5$ + FynKD	-41.9 [a]	0.5	5.4 [c]	0.5
$Na_v1.5$ + FynKD + BIM1	-41.5	0.5	5.6	0.6

[a] $P = .008$, [b] $P < .0005$, [c] $P = .021$

A) Normalized conductance as a function of membrane voltage. **Inset:** shows voltage protocol. Curves fitted with Boltzmann equation. B) Mean midpoint ($V_{1/2}$) values and C) Slope (k) values graphed. D) Table with $V_{1/2}$ and k values for each experiment. Matching superscript letters and asterisks signify statistical difference.

5.2. Steady-state Fast Inactivation

To test hypotheses 1-3, I measured steady-state fast inactivation. Cells were held at a holding potential of -130 mV, with alternating depolarizing steps ranging from -130 mV to +10 mV in 10 mV steps for duration of 500 ms. Current traces were not seen in the above pre-pulse potentials (Fig. 6). The test potential, at -10 mV for 19 ms, showed the number of channels that were available to activate after the specified pre-pulse potential (Fig. 7). Before each sweep, channels recovered from fast inactivation by a recovery pulse of -130 mV for 1 ms.

Figure 6. Steady-state fast inactivation current traces.

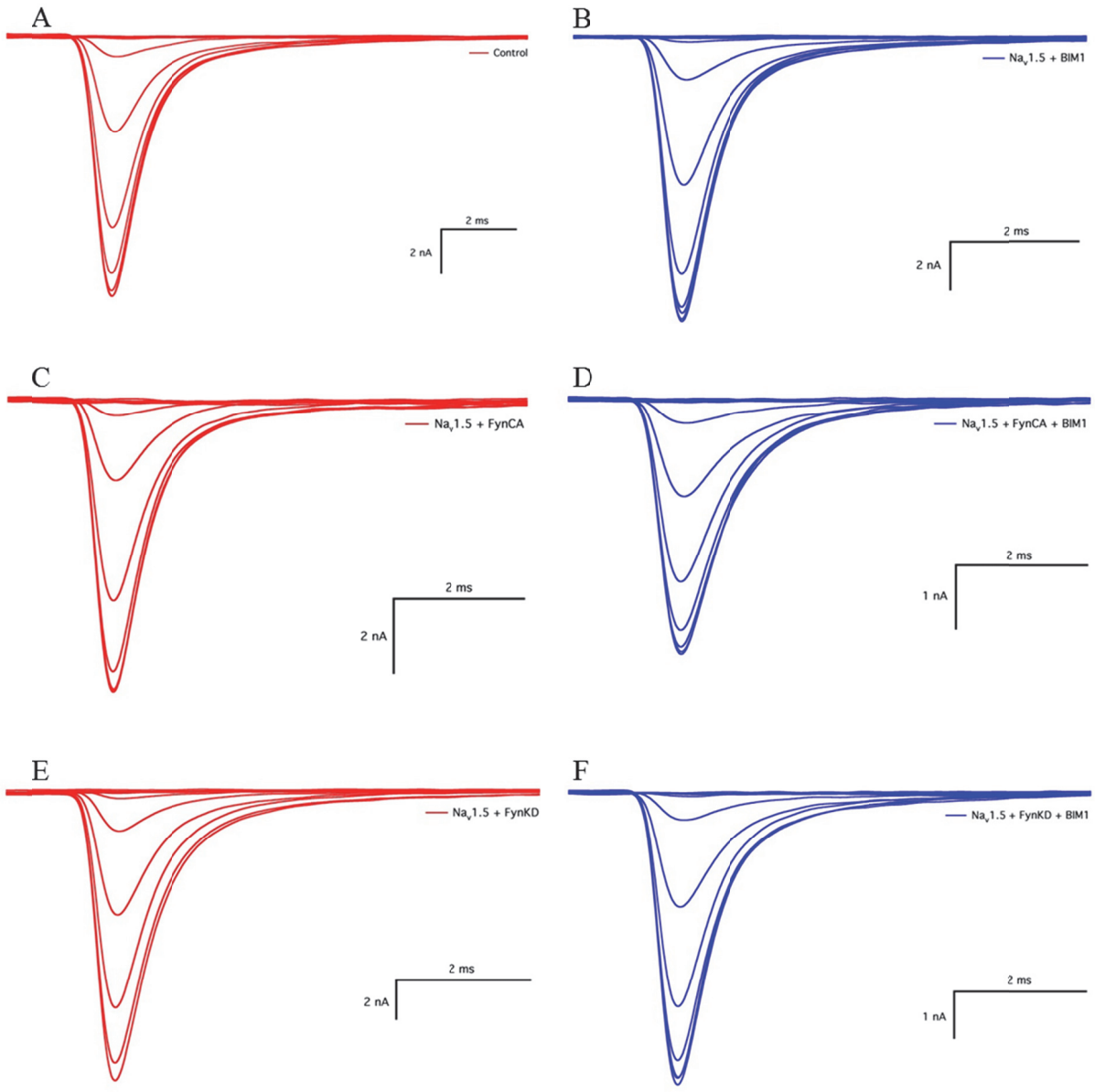

Representative current traces of the six experiments divided into two categories for clarification and comparison: (i) Without BIM1 (red) – which include A) control, C) Nav1.5 + FynCA and E) Nav1.5 + FynKD and (ii) With BIM1 (blue) – which include B) Nav1.5 + BIM1, D) Nav1.5 + FynCA + BIM1, and F) Nav1.5 + FynKD + BIM1.

The peak inward current was measured, normalized, plotted as a function of pre-pulse potential, and fitted with a Boltzmann equation (1) (Fig. 7). The mean $V_{1/2}$ of both $Na_v1.5$ + FynCA and $Na_v1.5$ + FynKD produced a significant hyperpolarizing shift compared to control (-7.1 mV and -3.6 mV respectively). $Na_v1.5$ + FynCA + BIM1

produced a significant +6.7 mV depolarizing shift compared to $Na_v1.5$ + FynCA. A depolarizing shift was also found in $Na_v1.5$ + FynKD + BIM1 versus $Na_v1.5$ + FynKD (+5.3 mV). The mean slope of $Na_v1.5$ + FynKD was steeper than $Na_v1.5$ + FynCA (-3.9 for both).

Figure 7. Steady-state fast inactivation.

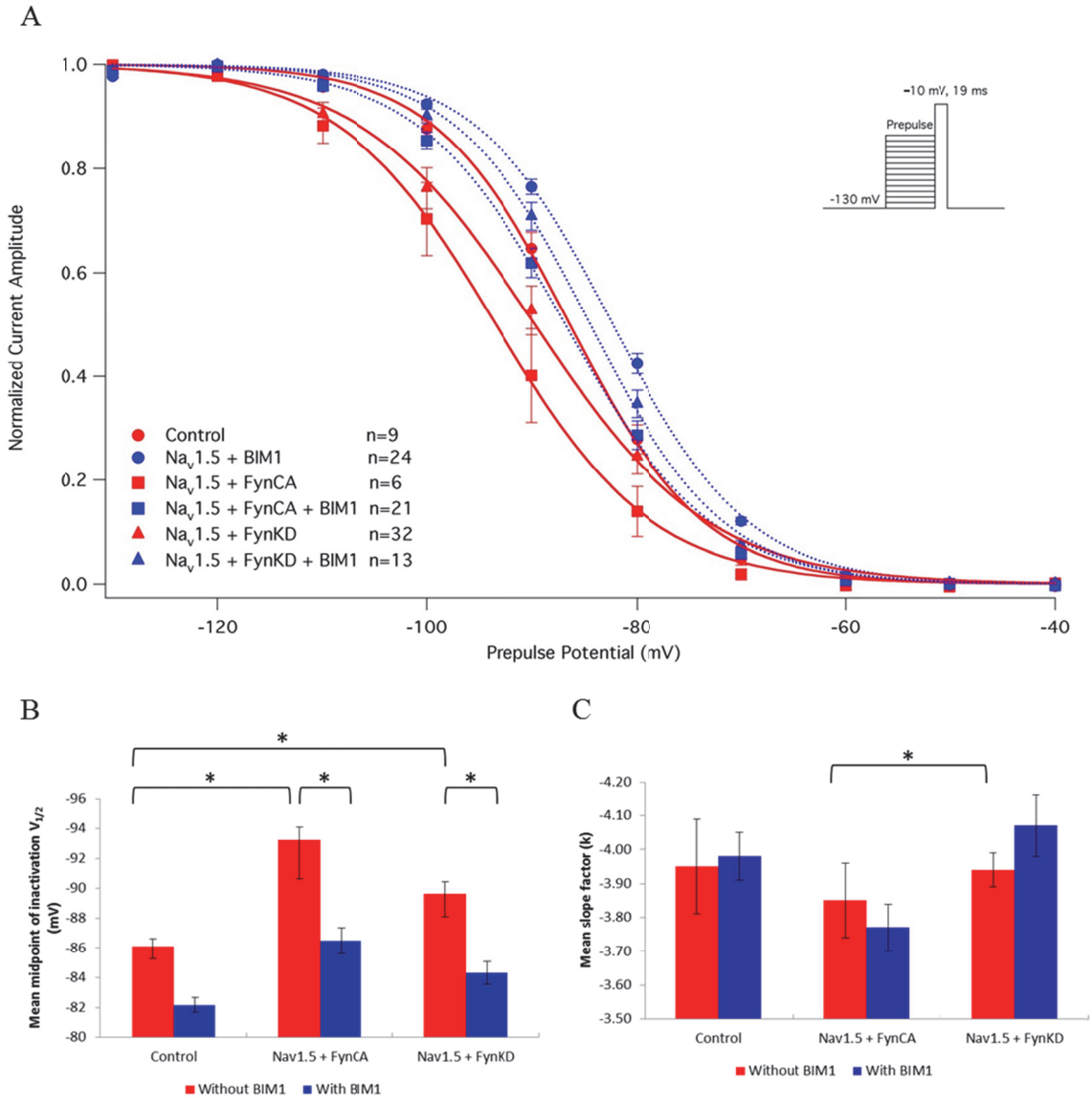

D

	Mean midpoint of inactivation $V_{1/2}$ (mV)	± SEM	Mean slope factor (k)	± SEM
Control	-86.1 [ab]	0.8	-4.0	0.1
$Na_v1.5$ + BIM1	-82.2	0.5	-4.0	0.1
$Na_v1.5$ + FynCA	-93.2 [ac]	2.6	-3.9 [e]	0.1
$Na_v1.5$ + FynCA + BIM1	-86.5 [c]	0.9	-3.8	0.1
$Na_v1.5$ + FynKD	-89.7 [bd]	1.6	-3.9 [e]	0.1
$Na_v1.5$ + FynKD + BIM1	-84.3 [d]	0.8	-4.1	0.1

[a] $P = .005$, [b] $P = .002$, [c] $P = 0.013$, [d] $P = .006$, [e] $P = .022$

A) Normalized current amplitude as a function of pre-pulse potential. Inset: shows voltage protocol. Curves fitted with Boltzmann equation. B) Mean midpoint ($V_{1/2}$) values and C) Slope (k) values graphed. D) Table with $V_{1/2}$ and k values for each experiment. Matching superscript letters and asterisks signify statistical difference.

5.3. Kinetics of Fast Inactivation

To measure recovery of $Na_v1.5$ from fast inactivation, I held the membrane potential at -130 mV for 500 ms prior to a step to 0 mV for 500 ms to fast inactivate channels. Recovery of current was measured during 19 ms pulse at -10 mV following 12 intervals of -130 mV (or -120, -110, -100, -90 mV) ranging from 0 to 1.02 s. Figure 8A shows recovery of fast inactivation as normalized current amplitude versus inter-pulse duration at -100 mV for all six experiments. Onset of fast inactivation was measured by stepping to a pre-pulse potential ranging from -90 mV to -30 mV from a holding potential of -130 mV for 500 ms. Current was measured during a 19 ms pulse at -10 mV following 12 intervals ranging from 0 to 1.02 s at the pre-pulse potential. Figure 8B shows onset of fast inactivation as normalized current amplitude versus pre-pulse duration at -80 mV for all six experiments. Time courses and the time constants for recovery and onset of fast inactivation data were fitted by a single exponential using equation (2) and were plotted as a function of membrane potential (Fig. 8C).

There was a statistical significant mean difference in time constants (i) between ENYZME ($P < .0005$), (ii) between mV ($P < .0005$) and (iii) the interaction term

ENZYME*mV ($P < .0005$). Post-hoc Tukey's test revealed significant difference in mean time constants between different levels of ENZYME: (i) $Na_v1.5$ + FynCA versus $Na_v1.5$ + FynCA + BIM1, (ii) $Na_v1.5$ + FynCA versus $Na_v1.5$ + FynKD, (iii) $Na_v1.5$ + FynCA versus $Na_v1.5$ + BIM1 and (iv) control versus $Na_v1.5$ + BIM1. Finally, there were statistical differences in mean time constant for each ENZYME level at: (i) -100 mV (ii) -80 mV, and (iii) -70 mV.

Figure 8. Kinetics of fast inactivation.

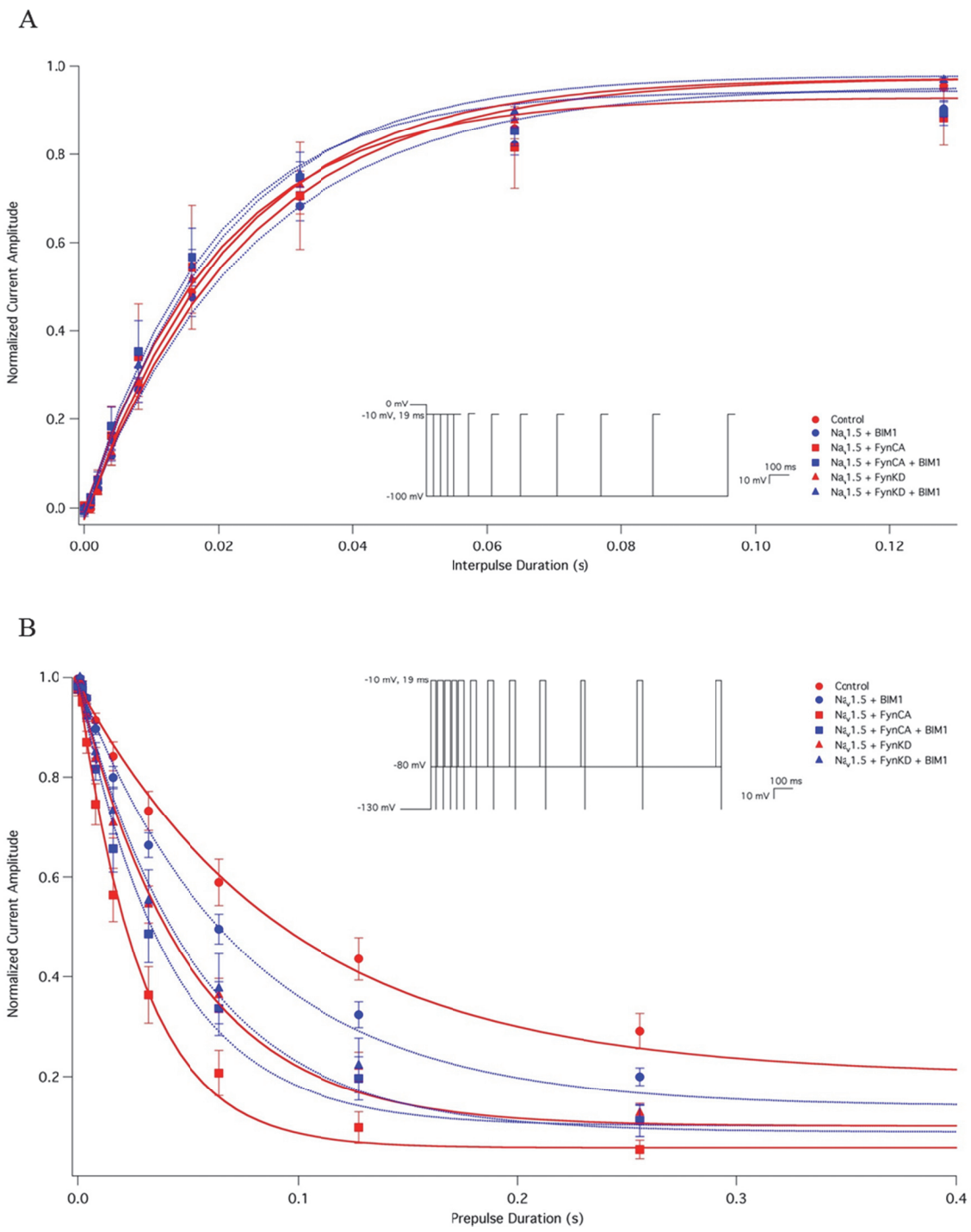

C

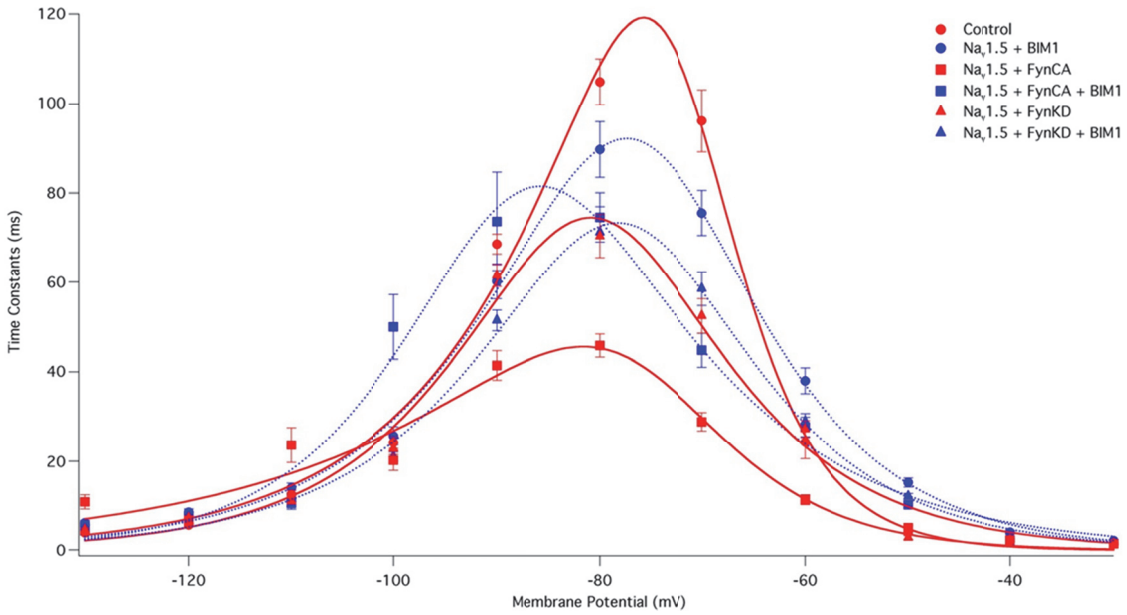

D

	Voltage (mV)	-100$^{\alpha}$	-80$^{\beta}$	-70$^{\gamma}$
Mean time constants (ms) ± SEM	Control^{d}	24.2 ± 1.3	104.9 ± 5.1	96.1 ± 7.0
	Nav1.5 + BIM1^{cd}	25.7 ± 2.1	89.7 ± 6.2	75.5 ± 5.0
	Nav1.5 + FynCA^{abc}	20.2 ± 2.3	45.8 ± 2.6	28.8 ± 2.0
	Nav1.5 + FynCA + BIM1^{a}	50.0 ± 7.2	74.5 ± 5.5	44.7 ± 3.8
	Nav1.5 + FynKD^{b}	22.7 ± 1.2	70.3 ± 4.9	52.4 ± 3.9
	Nav1.5 + FynKD + BIM1	21.0 ± 1.0	71.2 ± 5.7	58.5 ± 3.8

^{a} $P = .001$, ^{b} $P = .001$, ^{c} $P < .0005$, ^{d} $P < .0005$, $^{\alpha}$ $P = .027$, $^{\beta}$ $P < .0005$, $^{\gamma}$ $P < .0005$

A) Recovery of fast inactivation as normalized current amplitude as a function of interpulse duration. **Inset**: shows voltage protocol. B) Onset of fast inactivation as normalized current amplitude as a function of pre-pulse duration. **Inset**: shows voltage protocol. C) Time constants of recovery and onset of fast inactivation as a function of membrane potential. Representative traces without BIM1 (red) and with BIM (blue). Table D displays mean time constant values for voltages ranging from -100 mV, -80 mV, and -70 mV. Superscript symbols signify statistical difference between experimental group and Greek symbols signify statistical difference found within voltage group.

5.4. Open-state Fast Inactivation

To measure the voltage-dependence of open-state fast inactivation, I plotted time constants as a function of membrane potential. Time constants were derived from fitting single exponential fits on peak current (Fig. 4) to the end of the depolarizing pulse for each experiment. Only traces where a clear inward peak was visible (i.e. -50 mV to +10 mv) were measured. There was a significant difference in mean time constants (i) between ENZYME ($P < .0005$), (ii) between mV ($P < .0005$) and (iii) the interaction term ENZYME*mV ($P = .004$). No statistical differences in mean time constants between different levels of ENZYME were revealed by a post-hoc Tukey's test. Finally, there were statistical differences in mean time constants for each ENZYME level at (i) -50 mV and (ii) -40 mV.

Figure 9. Open-state fast inactivation.

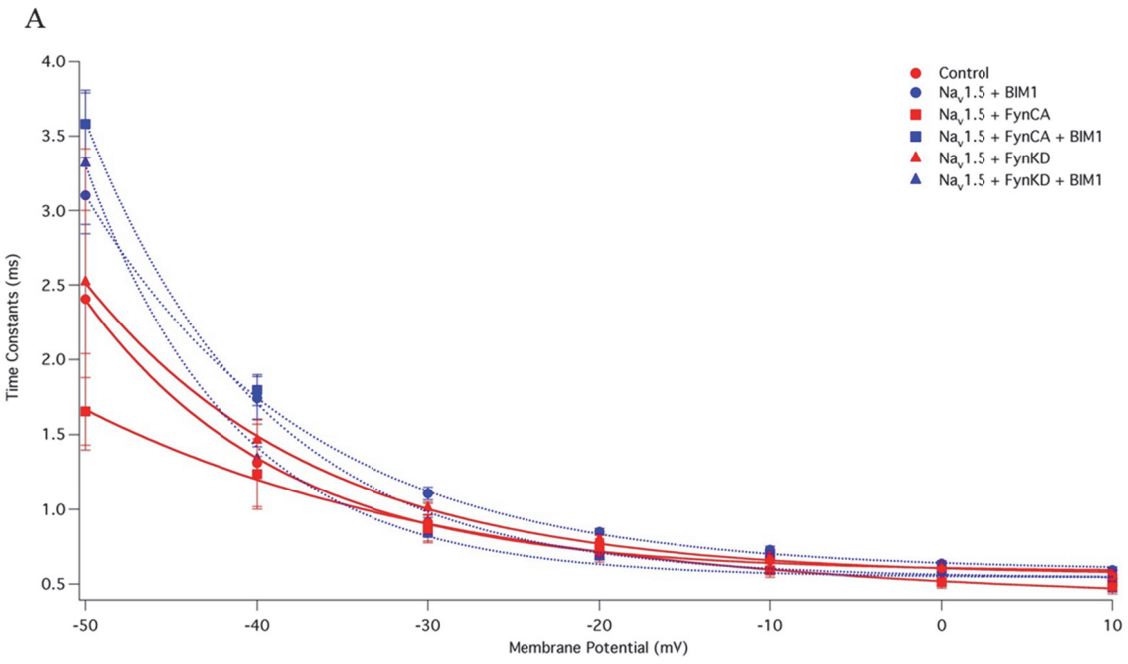

B

	Voltage (mV)	-50[α]	-40[β]	-30
Mean time constants (ms) ± SEM	Control	2.4 ± 1.0	1.3 ± 0.3	0.9 ± 0.1
	Nav1.5 + BIM1	3.1 ± 0.2	1.7 ± 0.1	1.1 ± 0.0
	Nav1.5 + FynCA	1.7 ± 0.2	1.2 ± 0.2	0.8 ± 0.1
	Nav1.5 + FynCA + BIM1	3.6 ± 0.2	1.8 ± 0.1	0.9 ± 0.0
	Nav1.5 + FynKD	2.5 ± 0.5	1.5 ± 0.1	1.0 ± 0.0
	Nav1.5 + FynKD + BIM1	3.3 ± 0.5	1.3 ± 0.1	0.9 ± 0.0

[α] $P < .0005$, [β] $P = .019$

A) Time constants of open-state fast inactivation as a function of membrane potential. Representative traces without BIM1 (red) and with BIM (blue). Table B displays mean time constant values for voltages ranging from -50 to -30 mV. Greek symbols signify statistical difference found within voltage group.

5.5. Window Current

Window current was measured from the overlap of steady-state activation and inactivation curves (see Figures 5 and 6). These curves were superimposed for each experimental condition, and the area encompassed by the two curves was calculated by integrating the area beneath the intersecting lines and measured in Arbitrary Units (AU, Table H). The values, therefore, were sensitive to the Boltzmann fit. As a result, the steady-state activation curves were adjusted for weight (standard deviation) to provide accurate values. Because of the derived nature of the measurement, significance testing and matched pairs were unavailable. Both Nav1.5 + FynCA and Nav1.5 + FynKD, however, appeared to increase the window current areas. No differences were observed between experimental conditions with BIM1, although all drug conditions have increased window current compared to the control.

Figure 10. Window Current.

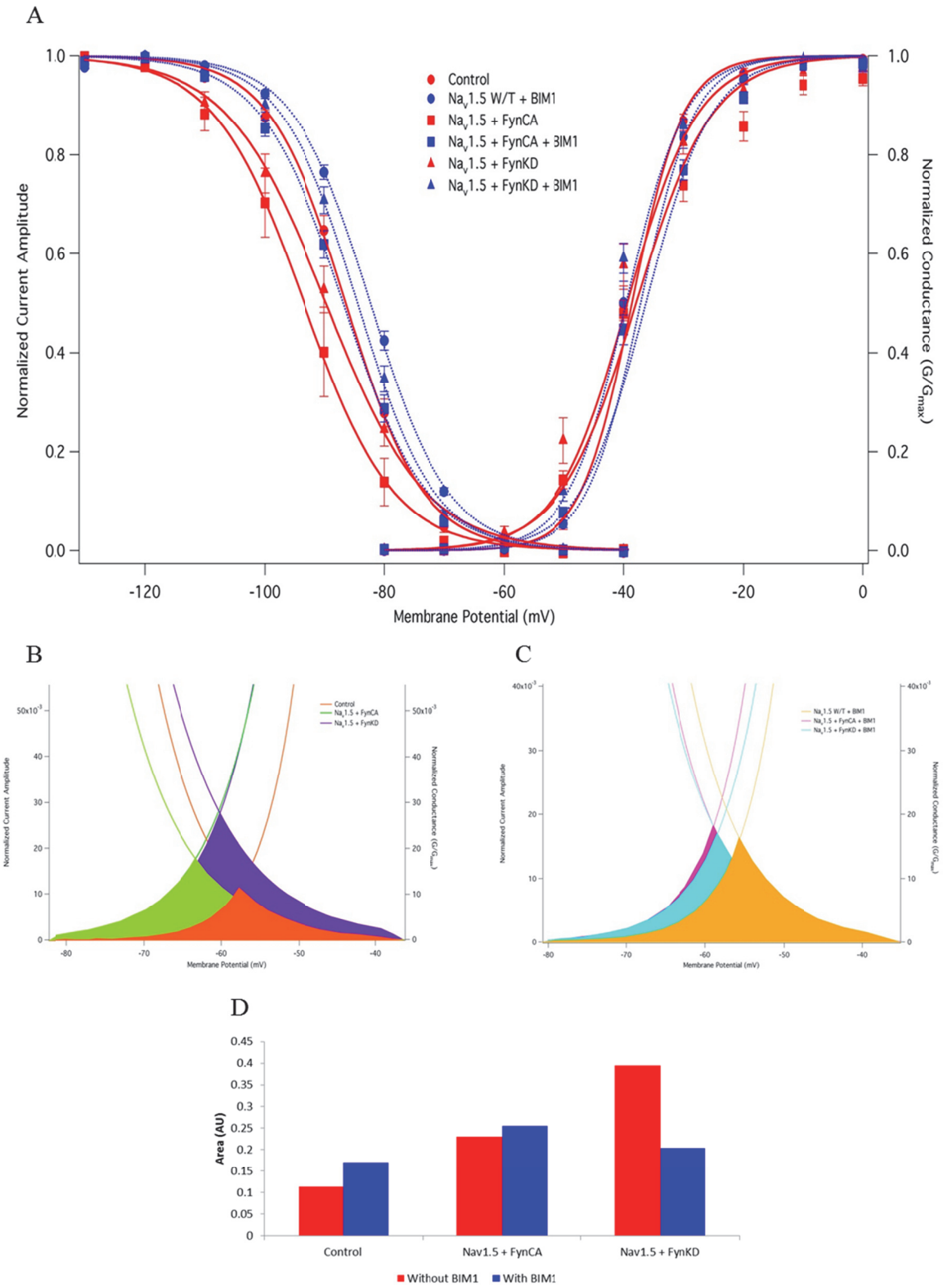

E

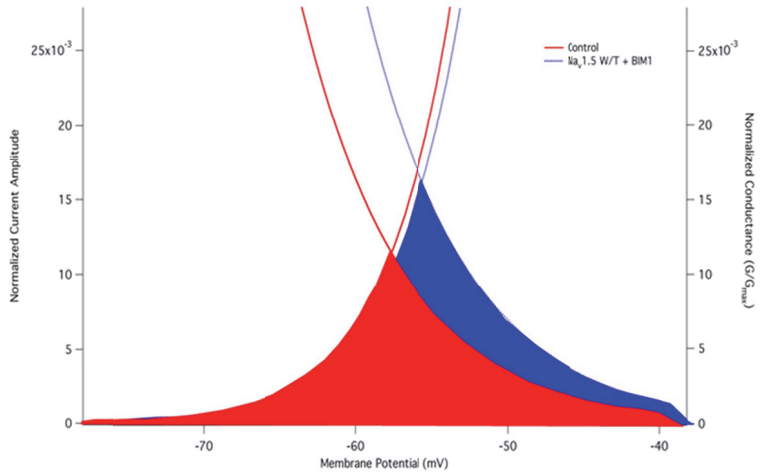
Control
Na$_v$1.5 W/T + BIM1
Normalized Current Amplitude
Normalized Conductance (G/G$_{max}$)
Membrane Potential (mV)
25x10^{-3}
20
15
10
5
0
-70
-60
-50
-40

F

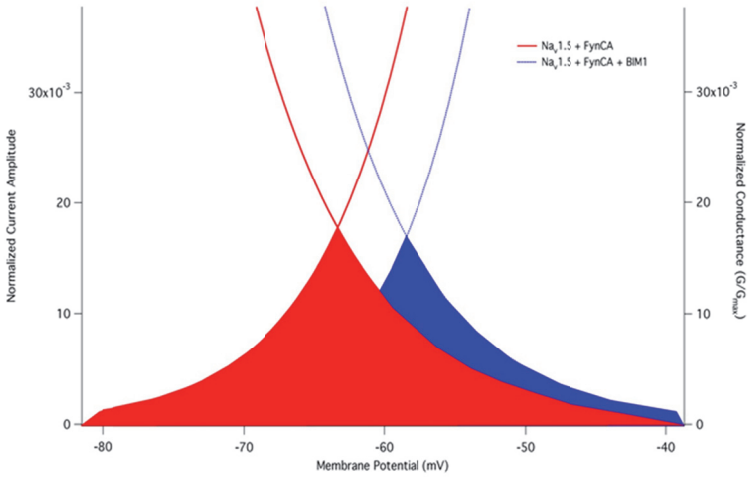
Na$_v$1.5 + FynCA
Na$_v$1.5 + FynCA + BIM1
Normalized Current Amplitude
Normalized Conductance (G/G$_{max}$)
Membrane Potential (mV)
30x10^{-3}
20
10
0
-80
-70
-60
-50
-40

G

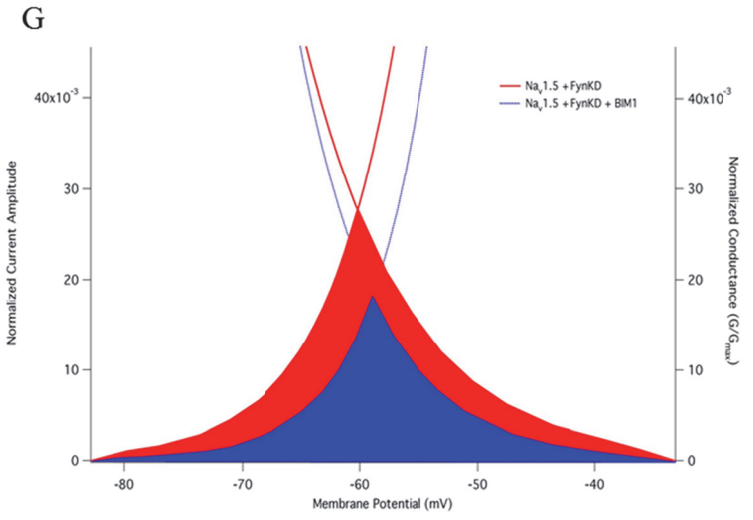
Na$_v$1.5 +FynKD
Na$_v$1.5 +FynKD + BIM1
Normalized Current Amplitude
Normalized Conductance (G/G$_{max}$)
Membrane Potential (mV)
40x10^{-3}
30
20
10
0
-80
-70
-60
-50
-40

H

	Area (AU)
Control	0.11
Nav1.5 + BIM1	0.17
Nav1.5 + FynCA	0.23
Nav1.5 + FynCA + BIM1	0.26
Nav1.5 + FynKD	0.40
Nav1.5 + FynKD + BIM1	0.20

A) Representative traces for window current by superimposing steady-state activation and inactivation curves. B) and C) depict window current area for experiments Without BIM1 and With BIM1 respectively. Experiments With BIM1 show area normalization. D), E), and F) depict area for pairwise comparisons between the control versus $Na_v1.5$ + BIM1, $Na_v1.5$ + FynCA versus $Na_v1.5$ + FynCA + BIM1, and $Na_v1.5$ + FynKD versus $Na_v1.5$ + FynKD + BIM1, respectively. $Na_v1.5$ + FynKD (Graph G and accompanying table H) showed the largest area and also the greatest change when treated with BIM1. Area did not change in $Na_v1.5$ + FynCA when compared to BIM1 treatment; however, BIM1 shifted the window current towards depolarized potentials. Significance testing was unavailable because comparisons did not represent matched pairs.

5.6. Action Potential Modeling

To visualize the effect of dual kinase modulation of $Na_v1.5$, a ventricular midmyocardial action potential model was generated. Figure 11A highlights action potentials for all six experimental conditions. Figure 11B is an expanded view of Figure 11A to show the action potential towards the end of the duration. Figures 11C and 11D illustrate the effect of dual kinase modulation on sodium current flowing during Phase 0 of the action potential at the beginning and towards the end of the action potential duration, respectively. $Na_v1.5$ + FynCA had a shortened action potential duration, decreased and delayed inward sodium current, and increased non-inactivating current compared to control (and all other experiments).

Figure 11. Action potential modeling of $Na_v1.5$.

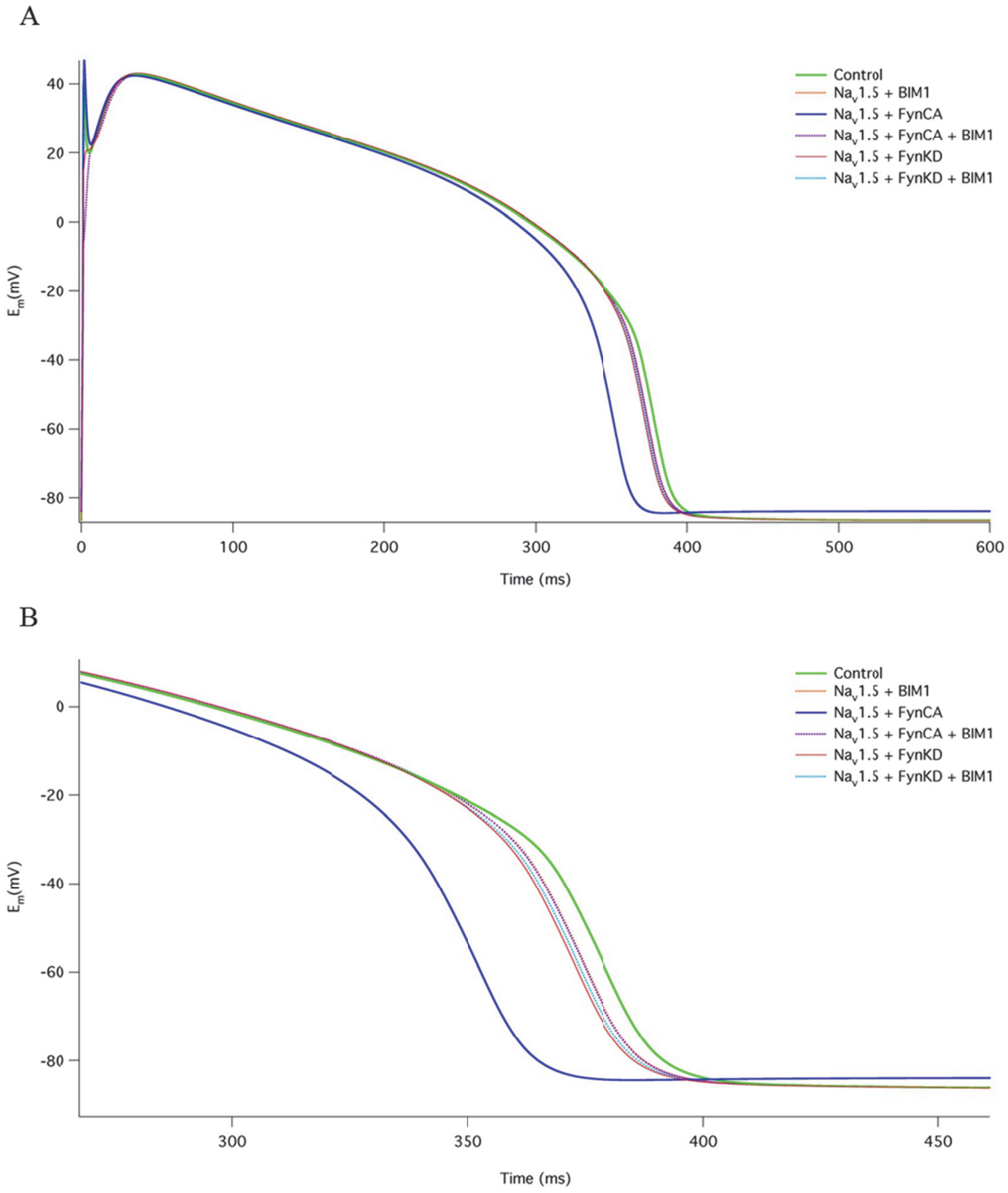

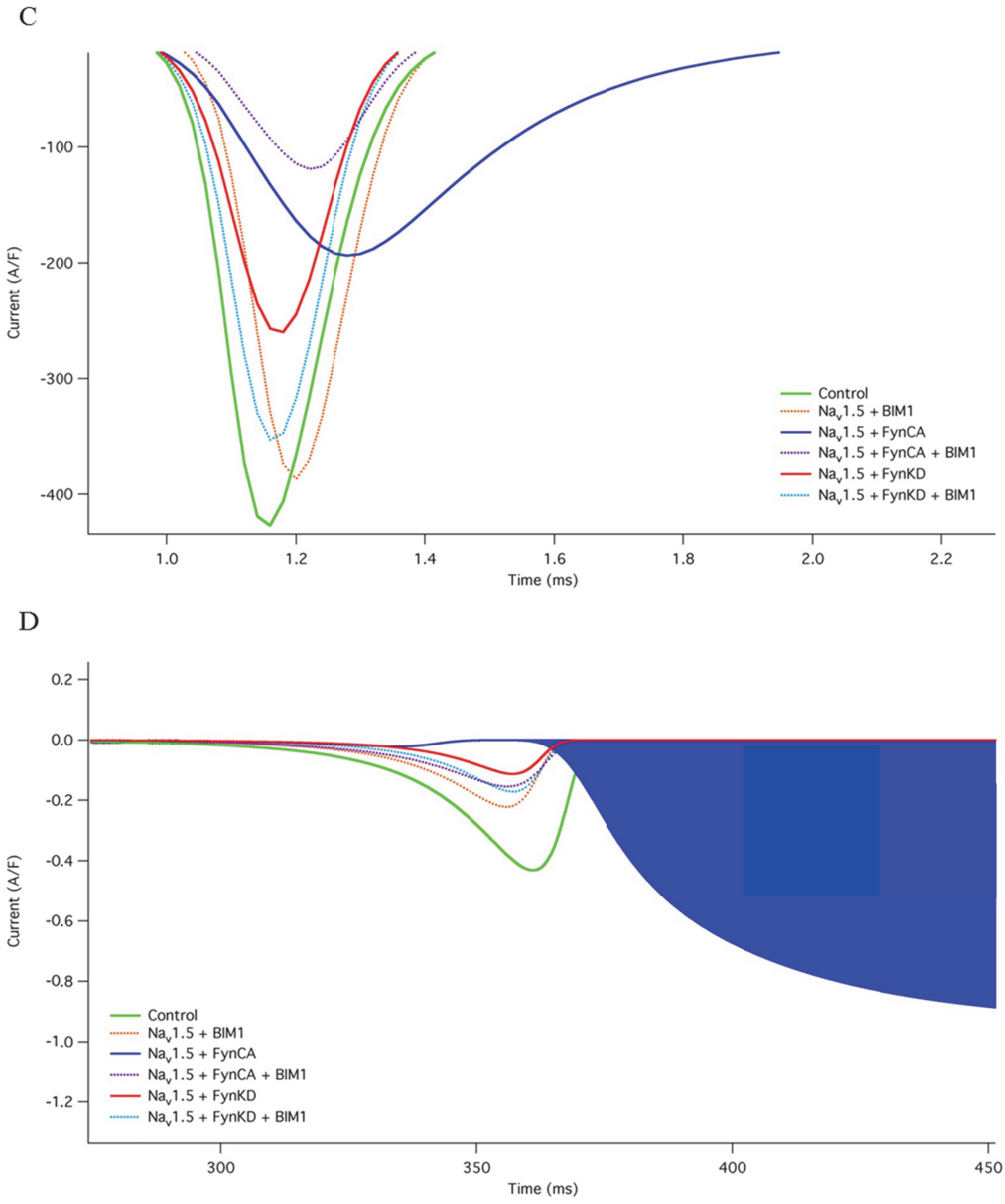

A) Midmyocardial action potential illustrating all six experimental conditions. B) $Na_v1.5$ + FynCA showed shortened action potential duration and non-inactivating current compared to control, $Na_v1.5$ + FynKD and With BIM1 group. Figures C) and D) show expanded views of Phase 0 (I_{Na}) of action potential. $Na_v1.5$ + FynCA showed (i) decreased and delayed inward sodium current and (ii) increased non-inactivating current compared to control and all other experiments.

6. Discussion

Basal phosphorylation of $Na_v1.5$ due to PKA, PKC, and Fyn kinase follows three separate signal transduction pathways. PKA and PKC activation occurs via G_s and G_q proteins of the GPCR pathway, respectively, and Fyn kinase activation occurs via integrin stimulation (Fig. 2A). During times of cardiac stress, cancer therapy, and growth, the constitutive activation of one or more of these enzymes induces the sharing of pathways (Fig. 2B) [38-40]. Re-routing signal transduction pathways may be due to energy conservation (by eliminating redundant proteins) or enzyme availability, thereby changing the modulation of target proteins. This study examined the dual kinase modulation of PKC and Fyn kinase on $Na_v1.5$ by using constitutively active or catalytically inactive mutants of Fyn kinase, and BIM1 (a partially selective PKC inhibitor). To validate the integration of PKC and Fyn kinase pathways (i) $Na_v1.5$ + FynCA would modulate the channel differently than control (basal phosphorylation of both Fyn and PKC) and (ii) $Na_v1.5$ + BIM1 (basal block of PKC and basal phosphorylation of Fyn). Furthermore, if constitutively active Fyn kinase induced dual kinase modulation of $Na_v1.5$, then the dominant-negative form, FynKD, would not be statistically significant from control, thereby strengthening my hypothesis. Finally, if blocking both tyrosine and S/T phosphorylation (as was the case in $Na_v1.5$ + FynKD + BIM1) is different than $Na_v1.5$ + FynCA, then it is plausible that dual kinase modulation is in effect. The results from my study show that Nav1.5 + FynCA (without BIM1) reduces excitability of cells compared to other experimental treatments, suggesting that (i) $Na_v1.5$ is differentially modulated by dual kinases (as compared to two independent pathways) and (ii) this modulation may contribute to cardiac (dys)function.

6.1. $Na_v1.5$ + FynCA reduces excitability

To test whether there was dual kinase modulation of $Na_v1.5$, HEK293 cells were co-expressed with a constitutively active mutant of Fyn kinase (FynCA) while PKC modulation of the channel remained intact. Compared to control, steady-state fast

inactivation curves (Fig. 7A) showed cells co-expressing $Na_v1.5$ + FynCA shifted in the hyperpolarizing direction. Time constants for the onset and recovery of fast inactivation were accelerated significantly for $Na_v1.5$ + FynCA (Fig. 8A, B). My results are consistent with Ahn et al., in which similar experiments used $Na_v1.2$ and Fyn kinase co-expression in tsA201 cells [35]. Ahn's study confirmed Fyn kinase modulation on neuronal sodium channels and co-expression yielded the same results (i.e. hyperpolarizing shift in the midpoint of steady-state fast inactivation, accelerated time constants and no changes in activation midpoint) [35]. The increase in tyrosine phosphorylation causes a larger fraction of sodium channels to remain in the inactivated state at resting membrane potential. This stabilization of the fast-inactivated state for Fyn kinase is also consistent with PKA and PKC studies as mentioned in the Introduction [26, 27, 35]. As a result, a larger stimulus would therefore be required to activate the channels so that the action potential can propagate to surrounding areas. The accelerated inactivation should reduce excitability by decreasing the inward sodium current (Fig. 11C) and shortening the action potential results in reduced calcium channel activation (Fig. 11A). While the modeling does not offer quantifiable data, the APD shortens when $Na_v1.5$ is co-expressed with an enzyme or a drug, however, only $Na_v1.5$ + FynCA shows a dramatic difference in APD. The delay in inward sodium current (Fig. 11C) results from the shifts noticed in steady-state activation and inactivation.

The hyperpolarizing shift in steady-state fast inactivation I observed has also been reported in PKC studies in which PKC was constitutively activated by OAG [26, 27]; steady-state fast inactivation curves for both $Na_v1.2$ and $Na_v1.4$ (the latter being expressed in cardiac myocytes), shifted in the negative direction [73-75]. PKC inhibitors removed/reduced this shift and no tyrosine inhibitors were used during these experiments [74, 75]. If both PKC and Fyn kinase studies (in $Na_v1.2$ at least) show negative shifts in steady-state inactivation and accelerated kinetics, then how do these results validate that PKC and Fyn kinase work in concert by sharing a signal transduction pathway? Strauss et al., studied dual kinase modulation of L-type calcium channel in retinal pigment epithelial (RPE) cells [39]. Briefly, RPE cells are involved in secreting growth factors and regulating photoreceptors in the eye. Perforated-patch clamp recordings of these cells revealed key results as indicated in the table below (Table 12). The study concluded three key points: (i) in cells with resting PKC activity,

the block of PTK led to a decrease in calcium current, (ii) in cells with stimulated PKC, block of PTK lead to an increase in calcium current, and (iii) the activity of PKC appears to dictate whether PTK reduces or enhances calcium currents. The authors of this study, therefore, suggest that dual kinase modulation differentially regulates L-type calcium channels. A subsequent study was conducted by the same authors, but this time, $K_v1.3$ (the primary delayed rectifying outward potassium channel) in RPE cells was studied and the same conclusions were found [76]. My experimental protocol uses the opposite situation (stimulating PTK, while blocking PKC), however Strauss et al., conducted experiments to conclude that the order of the kinase activation/block did not matter. If dual kinase modulation does indeed exist, then there should be differential results in my $Na_v1.5$ + FynCA + BIM1 experiments.

Table 12. Summary of RPE L-type calcium channel modulation.

Serine/Threonine		Tyrosine		Result
Activator	Inhibitor	Activator	Inhibitor	
-	-	-	Genistein	↓ current
-	-	-	Lavendustin A	↓ current
-	-	-	Diadzein[α]	No change
-	-	pp60[c-srcβ]	-	↑ current
-	H9[γ]	-	-	No change
-	H9 [γ]	-	Genistein	↓ current
-	Chelerythrine	-	-	↓ current
-	Calyculin[δ]	-	-	↑ current
-	Chelerythrine	-	Lavendustin A	↓ ↓current
-	Chelerythrine	-	Genistein	↓ ↓current
PMA	-	-	-	No change
PMA	Calyculin[δ]	-	-	↑ current
PMA	-	-	Genistein	↑ current
-	MARKCS[ε]	-	-	↑ current
-	MARKCS[ε]	pp60[c-srcβ]	-	↑ current
PMA	-	pp60[c-srcβ]	-	↓ current

[α] inactive analog of Genistein, [β] Src kinase, [γ] PKA/PKG inhibitor, [δ] S/T phosphatase inhibitor, [ε] myristoylated PKC

Activators and inhibitors of S/T and/or tyrosine kinases were applied to the channel. Rows highlighted in blue depict the change in channel modulation when PKC is stimulated or blocked (and tyrosine kinases were blocked). Rows highlighted in red show stimulation of tyrosine kinases (when PKC is activated or blocked). The modulation of the channel changes which is indicative of the integration of the two kinase pathways [39].

Since cells co-expressing $Na_v1.5$ + FynCA confer faster kinetics, more channels are available for activation for the next depolarization; there is an increased probability of channels that are transitioning in and out of inactivated states resulting in non-inactivating current (Figure 11D). Window current analysis (Fig. 10F) showed a larger area for $Na_v1.5$ + FynCA compared to control especially at resting membrane potential. A larger window current may result in increased excitability and, therefore, may be pro-arrthymogenic [77]. These cells also do not reach resting membrane potential after each cycle (Fig. 11B), which suggests there are channels already activated before the next depolarization, as suggested by the window current analysis. Compared to control, these results suggest that $Na_v1.5$ + FynCA may be pro-arrthymogenic because the midmyocardium should normally be in refractory. Therefore, the non-inactivating current increases the susceptibility of errant depolarizations [78]

6.2. $Na_v1.5$ + FynCA + BIM1 does not affect excitability

This study used BIM1, a partially-selective PKC inhibitor, to determine whether PKC and Fyn kinase modulate $Na_v1.5$ by the same downstream pathway. The results for $Na_v1.5$ + FynCA would therefore be different when compared to $Na_v1.5$ + FynCA + BIM1, to show that without PKC, the modulation of $Na_v1.5$ is different. As mentioned above, Ahern et al., co-expressed $Na_v1.5$, FynCA, and BIM1 in HEK293 cells [29]. Although there was no change in the midpoint or slope of activation (consistent with my results), a depolarizing shift from control was observed in the steady-state fast inactivation midpoint. In contrast, my results demonstrate that $Na_v1.5$ + FynCA + BIM1 depolarized the steady-state inactivation curve compared to $Na_v1.5$ + FynCA, but this shift was not significant when compared to control or $Na_v1.5$ + BIM1 (Fig. 7A). Although Ahern's results seem inconsistent with my study, their study did not include experiments without BIM1. Furthermore, the conclusions from Ahern's study were based on hyperpolarizing shifts in steady-state inactivation curves when tyrosine inhibitors were applied to isolated cardiac myocytes [79]. As noted in the study limitations section, Fyn kinase modulates several ion channels, including $I_{K(ATP)}$, I_{Ks}, I_{Kr}, I_{Kur} [68-70]. PKC modulates other ion channels, such as I_{Ks}, I_{to}, I_{CaL} [14, 71, 72]. Although these lists are not exhaustive, they indicate the complexities associated with ion channel

phosphorylation and the possibility of over-interpreting results, especially when comparing heterologous expression systems to cardiomyoctes. Furthermore, the tyrosine inhibition study on cardiomyocytes by Wang et al., (i) did not constitutively activate any tyrosine kinases, (ii) the drugs used in the study Genistein and Tyrphostin AG 957 target non-Src family kinases (epidermal growth factor receptor – EGFR and Bcr-Abl respectively) and (iii) used CsF in the internal pipette solution [79]. The issues using CsF in heterologous expression systems has been addressed, but the effect can be amplified in cardiomyocytes as numerous kinases are modulating numerous channels. Therefore the extent to which Fyn kinase (and Src kinase family) is effectively being blocked and contributing to the shift in steady-state inactivation is questionable.

In this study, significant differences were not found between the midpoint and slope of steady-state inactivation between $Na_v1.5$ + FynCA + BIM1 and control (or $Na_v1.5$ + BIM1). $Na_v1.5$ + FynCA + BIM1 showed significantly slower time constants for the voltage-dependence of inactivation (when compared to $Na_v1.5$ + FynCA) which suggests that the addition BIM1 prevented and/or reduced hypoexcitability (Fig. 8C). Window current analysis for $Na_v1.5$ + FynCA + BIM1 showed similar but depolarizing shift compared to $Na_v1.5$ + FynCA (Fig. 10F). However, when compared to all other BIM1 treatments, there does not seem to be any noticeable differences, rather the drug normalizes window current (Fig. 10C); the application of BIM1 stabilizes the window current perhaps providing a protective effect in the event where other enzymes may promote pathogenic behaviour. Interestingly, BIM1 and its derivatives, MS1 (2-[1-(3-aminopropyl)indol-3-yl]-3-(indol-3-yl)-N-methylmaleimide) have been shown to be cardioprotective [80]. MS1 was applied to rat myocardium, in vivo, before ischemia and after reperfusion and reduced the occurrence of ventricular fibrillation and infarct size. Action potential modeling is consistent with window current analysis. $Na_v1.5$ + FynCA + BIM1 does not shorten the action potential duration, however, there is reduced inward sodium current even more so than $Na_v1.5$ + FynCA (Fig. 11B, C). The decreased inward sodium drive may be due to greater access given to Fyn kinase to either (i) buried tyrosine residues or (ii) tyrosine residues nearby S/T residues that are not being phosphorylated by PKC. As a result, the increase in non-inactivating current was caused by Fyn kinase modulation and not by PKC phosphorylation.

6.3. Down-regulation of Fyn kinase ($Na_V1.5$ + FynKD) does not affect excitability

The co-expression of FynKD drives major changes in ion channel modulation. The ratio of dead kinase is greater than endogenous kinase thereby shifting the equilibrium towards reducing the probability the channel will be tyrosine-phosphorylated (even beyond basal levels). As a result, FynKD competes with endogenous Fyn kinase by competing for binding sites blocking potential tyrosine residues from being phosphorylated. No change in activation was observed in cells co-expressing $Na_V1.5$ + FynKD when compared to control (Fig. 5A). $Na_V1.5$ + FynKD cells exhibited slower recovery and onset of fast inactivation compared to $Na_V1.5$ + FynCA (Fig 8C). The midpoint of inactivation, however, shifted in the hyperpolarizing direction when compared to control (Fig. 7A). This observation is interesting, since the same (albeit larger) results were observed cells expressing $Na_V1.5$ + FynCA. Since phosphorylation is a dynamic interplay between kinases and phosphatases, this result is not completely unexpected. It is possible that PKC phosphorylation is compensating for the lack of tyrosine phosphorylation because (i) PKC can access residues near tyrosine residues which it normally cannot phosphorylate or (ii) because tyrosine modulation is being down-regulated, the stabilization is due to the cells compensatory mechanism (as completely inactive tyrosine kinases are not usually found in physiological settings). Both of these phenomenon can be explained by previous signal transduction studies. In 1999, Edwards et al., studied PKCβII in COS7 cells (CV-1 (simian) in Origin and carrying the SV40 genetic material) to show that T641 of PKCβII needs to be phosphorylated in order to activate the catalytic activity of the kinase [81]. Mutation of this consensus site causes nearby threonine residues to assume responsibility to compensate for the mutation. The K299M mutation in FynKD prevents catalytic activity. There are residues upstream of Y531 that could take on the role of activating the enzyme (Y523 or Y515) [33]. In my $Na_V1.5$ + FynKD experiments, then, not only does PKC have access to S/T residues, but also FynKD may still be catalytically active thereby phosphorylating tyrosine residues. In addition, Seig et al., studied the compensatory mechanism in FAK deficient mice [82]. Briefly, Focal Adhesion Kinase (FAK) is a PTK that links integrin to its signal transduction pathways proteins. The study by Seig expressed deficient FAK (FAK^-) in mice and found that Pyk2 (Protein tyrosine kinase 2) was upregulated to

compensate for the cells lack FAK. While Pyk2 is not as effective linking integrins to its transduction pathways, the pathway was not abolished in these mice.

However, the results from my study may also highlight the importance of PKC and S/T phosphorylation; it is plausible that (i) S/T phosphorylation blocks tyrosine phosphorylation (steric hindrance), or that (ii) S/T phosphorylation masks the effect of tyrosine phosphorylation (nearby negative charge from phosphorylated S/T residues may not be energetically favourable for Fyn kinase to phosphorylate a tyrosine residue (i.e. electrostatic hindrance)). Previous results showed that $Na_v1.5$ + FynKD + BIM1 shifts steady-state inactivation midpoint towards more negative potentials [29]. I observed that $Na_v1.5$ + FynKD + BIM1 depolarized the midpoint of steady-state inactivation. Although these results seem contradictory, it is plausible that PKC is still active and modulating the channel and stabilizing it in $Na_v1.5$ + FynKD cells. The lack of PKC destabilizes (as represented by a right shift in the steady-state inactivation curve) the channel.

As previously mentioned, the study by Ahern et al., used CsF in the internal pipette solution [29]. It is possible that although FynKD and BIM1 both inhibit tyrosine and S/T phosphorylation, respectively, fluoride may shift the equilibrium by activating any remaining kinases, resulting in channel modulation. Other kinases that regulate $Na_v1.5$, such as PKA and CaMKII may also be activated by fluoride via inhibition of S/T phosphatases [1, 56, 59]. The resulting phosphorylation may stabilize the channel due to the additional negative charge. Ahern et al. tried to solve this problem by using perforated-patch clamp (using CsCl instead) and tyrosine kinase inhibitors PP2 and Tyrphostin AG957. The perforated-patch results were consistent with the whole-cell experiments using CsF. The introduction of the two inhibitors not used in the whole-cell experiments, however, may complicate the effect of FynKD on Nav1.5 by introducing an additive effect (competition due to FynKD and complete block due to inhibitors) [39]. At the same time, the significant result observed by Ahern only compares $Na_v1.5$ + FynKD versus $Na_v1.5$ + FynCA; the midpoint and slope values for $Na_v1.5$ alone (control) were not reported. In my study, window current for $Na_v1.5$ + FynKD was much larger compared to $Na_v1.5$ + FynKD + BIM1 (Fig. 10G). This large window current may result in non-inactivating current, although action potential modeling did not confirm this speculation (Fig. 11A, B, D). The co-expression of either kinase or the application of

BIM1 shortened the action potential duration, but this could be due to the introduction of enzymes and/or drugs (Fig. 11A). Both FynKD experiments exhibited reduced inward sodium current (Fig. 11C) but not as significant as $Na_v1.5$ + FynCA. It is interesting to speculate that $Na_v1.5$ + FynKD may be pro-arrhythmogenic compared to complete block of phosphorylation ($Na_v1.5$ + FynKD + BIM1). It is possible that PKC modulation has a cardioprotective effect which is consistent with cardiac myocyte studies [14, 83].

6.4. Speculation about physiological significance

The physiological significance of dual kinase modulation has been reported by a number of previous studies. For example, the dual roles of PKC and PTK have been studied in ischemic preconditioning [84]. Briefly, preconditioning protects the myocardium in the early and late phase. The early phase protection begins immediately and can last up to 2-4 hours after ischemia, while the late phase begins 1-2 days later and can last 3-4 days after ischemic insult. Several proteins are involved in the preconditioning process, including nitric oxide (NO), reactive oxygen species (ROS), and PKC [83]. The α and ε isoforms of PKC have been shown to be involved in cardioprotection by forming complexes with Src family kinase to protect against hypertrophy and ischemia [14]. The study showed that inhibition of PTK's by Genistein and Lavendustin A blocked the activation of the above proteins. The inhibition of cardioprotection suggests that PKC and PTK share similar downstream pathways during times of cardiac stress. These results also suggest dual kinase modulation.

In 2009, Hsu et al., showed that reperfusion releases significant amounts of oleic acid (OA) from the myocardium [38]. This fatty acid, which is found in high concentrations in the lipid bilayer, leads to in vitro electrical uncoupling of cardiac myocytes by stimulating and activating PKC α, ε and Src family kinases (Fyn kinase). With the release of OA, however, activation of these two enzymes disrupts gap junction and adherens junction formation. PKC specific inhibitors, Gö 6976 and εV1-2, prevented both PKC and Fyn phosphorylation. Protein phosphatase 2 (PP2), a Src kinase specific inhibitor, prevented Fyn phosphorylation, suggesting Fyn activation is downstream of PKC.

The extent of dual kinase modulation can be seen in drug studies as well. Integrin and Fyn kinase signaling pathway is activated during insulin regulation [85, 86]. SU6656, is a Src-family kinase specific inhibitor that can also mimic Fyn kinase deficiency (Fyn^-) and is being studied as a potential weight-loss drug. The drug has been shown to decrease adipose mass while maintaining lean tissue mass. The drug assists in improving (i) insulin sensitivity, (ii) plasma and tissue triglyceride fatty acids levels, (iii) and increases the rate of energy expenditure and fatty acid oxidation in the fasted state. In addition to inhibiting Fyn kinase, SU6656 has been shown to inhibit PKCδ which is downstream of Fyn kinase; again, emphasizing the interaction and integration of these two enzymes.

Finally, anti-cancer drugs such as dasatinib (Sprycel) have been shown to be effective against Chronic Myelogenous Lekemia (CML) by inhibiting Src family tyrosine kinase [40]. Cardiotoxicity such as left ventricular (LV) dysfunction, heart failure (HF), generalized edema, and arrhythmias are the main side-effects of this drug [40]. Quinidine, an anti-arrhythmic agent, prolongs the QT interval (found on ECG) to prevent/reduce ventricular fibrillation [87]. Patients combining Quinidine with Sprycel have shown further increases in QT prolongation which, incidentally, is pro-arrhythmogenic [87].

7. Conclusions

The structure, function, and regulation of voltage-gated ion channels is critical for the successful propagation of action potentials. Numerous factors (i.e. channel mutations, drugs, pH, or temperature) may impair channel properties, leading to pathophysiological conditions. Phosphorylation modulates channel activity. Cardiac events such as ischemia and reperfusion result in the activation of tyrosine kinases which are involved in many signaling cascades that may lead to either cardioprotection or arrhythmogenesis. Here, I studied the constitutive activation of Fyn kinase in $Na_v1.5$ using HEK293 cells to understand a putative biophysical mechanism that may be involved in cardiac pathogenesis. The activation of kinases results in the sharing of downstream signaling pathways. This result was seen in $Na_v1.5$ + FynCA (without BIM1) compared to control, $Na_v1.5$ + FynCA + BIM1 and other experimental treatments. The change in kinetics and voltage-dependence infers differential modulation of $Na_v1.5$ as compared to basal level and single kinase modulation. The hypoexcitability of $Na_v1.5$ + FynCA (without BIM1) may be pro-arrhythmogenic as indicated by action potential modeling. This study, therefore, highlights the importance of post-translational modifications on voltage-gated ion channels, and provides novel insights into possible molecular mechanisms which may be involved in the pathophysiology of cardiovascular disease.

8. Future Directions

The dynamic interplay between kinases and phosphatases on target proteins prompts continued study. This study shows that activation of kinases can change ion channel kinetics (when compared to basal levels), and that the effects may be pathophysiological. As mentioned in the study limitations, including β-subunits (actively) in future studies would be the logical next step. In 2009, Lin et al., studied constitutively active Fyn kinase (FynY531F) on HCN4 pacemaker channel mutant (D553N) [88]. The channel mutant reduced surface expression on the plasma membrane and the active Fyn increased mutant trafficking. It is plausible, that FynCA also affects $Na_v1.5$ trafficking that may differ from, or be in parallel with, β co-expression. Further studies might include Fyn kinase regulation in SCN5A channelopathies such as LQT and Brugada Syndrome (BrS), especially those with tyrosine-related mutations.

It would be interesting to study dual PKC and Fyn kinase modulation in cardiac myocytes. To study voltage gated sodium channels, several blockers must be applied to eliminate current from other channels (and TTX can be used to select for $Na_v1.5$ from other Na_v isoforms). The results from my study could then be compared to this future cardiomyocyte study to determine whether (i) there is a change in channel kinetics and voltage-dependence, and (ii) what can be inferred physiologically from the difference in expression systems. Fyn kinase modulation of sodium channels in cardiomyocytes could be further evaluated using co-localization studies to show (i) time-dependent PKC and Fyn kinase modulation or (ii) protein complex formation using fluorescence.

Finally, it would be interesting to study the cardiotoxic effects of the anti-cancer drugs mentioned above, since the drugs either activate or block kinases which induce signal transduction pathways that are normally quiescent.

9. Reference List

1. Scheuer, T., *Regulation of sodium channel activity by phosphorylation.* Semin Cell Dev Biol, 2010.
2. Abriel, H., *Roles and regulation of the cardiac sodium channel Na v 1.5: recent insights from experimental studies.* Cardiovasc Res, 2007. **76**(3): p. 381-9.
3. Fozzard, H.A., P.J. Lee, and G.M. Lipkind, *Mechanism of local anesthetic drug action on voltage-gated sodium channels.* Curr Pharm Des, 2005. **11**(21): p. 2671-86.
4. Anderson, P.A., M.A. Holman, and R.M. Greenberg, *Deduced amino acid sequence of a putative sodium channel from the scyphozoan jellyfish Cyanea capillata.* Proc Natl Acad Sci U S A, 1993. **90**(15): p. 7419-23.
5. Yu, F.H., et al., *Overview of molecular relationships in the voltage-gated ion channel superfamily.* Pharmacol Rev, 2005. **57**(4): p. 387-95.
6. Payandeh, J., et al., *The crystal structure of a voltage-gated sodium channel.* Nature, 2011. **475**(7356): p. 353-8.
7. Yu, F.H., et al., *Sodium channel beta4, a new disulfide-linked auxiliary subunit with similarity to beta2.* J Neurosci, 2003. **23**(20): p. 7577-85.
8. Catterall, W.A., *From ionic currents to molecular mechanisms: the structure and function of voltage-gated sodium channels.* Neuron, 2000. **26**(1): p. 13-25.
9. Marban, E., T. Yamagishi, and G.F. Tomaselli, *Structure and function of voltage-gated sodium channels.* J Physiol, 1998. **508 (Pt 3)**: p. 647-57.
10. Isom, L.L., *Sodium channel beta subunits: anything but auxiliary.* Neuroscientist, 2001. **7**(1): p. 42-54.
11. Ashcroft, F.M., *Ion channels and disease : channelopathies*. 2000, San Diego: Academic Press. xxi, 481 p.
12. Hille, B., *Ion channels of excitable membranes*. 3rd ed. 2001, Sunderland, Mass.: Sinauer. xviii, 814 p., [8] p. of plates.
13. Bosmans, F., M.F. Martin-Eauclaire, and K.J. Swartz, *Deconstructing voltage sensor function and pharmacology in sodium channels.* Nature, 2008. **456**(7219): p. 202-8.
14. Bers, D.M., *Excitation-contraction coupling and cardiac contractile force*. 2nd ed. Developments in cardiovascular medicine. 2001, Dordrecht ; Boston: Kluwer Academic Publishers. xxiv, 427 p.
15. Errington, A.C., T. Stohr, and G. Lees, *Voltage gated ion channels: targets for anticonvulsant drugs.* Curr Top Med Chem, 2005. **5**(1): p. 15-30.

16. Catterall, W.A., A.L. Goldin, and S.G. Waxman, *International Union of Pharmacology. XLVII. Nomenclature and structure-function relationships of voltage-gated sodium channels.* Pharmacol Rev, 2005. **57**(4): p. 397-409.

17. Roden, D.M. and A.L. George, Jr., *Structure and function of cardiac sodium and potassium channels.* Am J Physiol, 1997. **273**(2 Pt 2): p. H511-25.

18. Molleman, A. and MyiLibrary., *Patch clamping an introductory guide to patch clamp electrophysiology*. 2003, J. Wiley: New York. p. x, 175 p.

19. Garrett, R. and C.M. Grisham, *Biochemistry*. 4th ed. 2010, Boston, Mass.: Brooks/Cole. 1 v. (various pagings).

20. Cantrell, A.R. and W.A. Catterall, *Neuromodulation of Na+ channels: an unexpected form of cellular plasticity.* Nat Rev Neurosci, 2001. **2**(6): p. 397-407.

21. Beacham, D., et al., *Sites and molecular mechanisms of modulation of Na(v)1.2 channels by Fyn tyrosine kinase.* J Neurosci, 2007. **27**(43): p. 11543-51.

22. Matsuda, J.J., H. Lee, and E.F. Shibata, *Enhancement of rabbit cardiac sodium channels by beta-adrenergic stimulation.* Circ Res, 1992. **70**(1): p. 199-207.

23. Tateyama, M., et al., *Modulation of cardiac sodium channel gating by protein kinase A can be altered by disease-linked mutation.* J Biol Chem, 2003. **278**(47): p. 46718-26.

24. Mellor, H. and P.J. Parker, *The extended protein kinase C superfamily.* Biochem J, 1998. **332 (Pt 2)**: p. 281-92.

25. Glazer, R.I., *The protein kinase ABC's of signal transduction as targets for drug development.* Curr Pharm Des, 1998. **4**(3): p. 277-90.

26. Qu, Y., et al., *Modulation of cardiac Na+ channels expressed in a mammalian cell line and in ventricular myocytes by protein kinase C.* Proc Natl Acad Sci U S A, 1994. **91**(8): p. 3289-93.

27. Qu, Y., et al., *Phosphorylation of S1505 in the cardiac Na+ channel inactivation gate is required for modulation by protein kinase C.* J Gen Physiol, 1996. **108**(5): p. 375-9.

28. Tateyama, M., et al., *Stimulation of protein kinase C inhibits bursting in disease-linked mutant human cardiac sodium channels.* Circulation, 2003. **107**(25): p. 3216-22.

29. Ahern, C.A., et al., *Modulation of the cardiac sodium channel NaV1.5 by Fyn, a Src family tyrosine kinase.* Circ Res, 2005. **96**(9): p. 991-8.

30. Jespersen, T., et al., *Cardiac sodium channel Na(v)1.5 interacts with and is regulated by the protein tyrosine phosphatase PTPH1.* Biochem Biophys Res Commun, 2006. **348**(4): p. 1455-62.

31. Yang, S. and B. Roux, *Src kinase conformational activation: thermodynamics, pathways, and mechanisms.* PLoS Comput Biol, 2008. **4**(3): p. e1000047.

32. Tatosyan, A.G. and O.A. Mizenina, *Kinases of the Src family: structure and functions.* Biochemistry (Mosc), 2000. **65**(1): p. 49-58.

33. Kinoshita, T., et al., *Structure of human Fyn kinase domain complexed with staurosporine.* Biochem Biophys Res Commun, 2006. **346**(3): p. 840-4.

34. Dorn, G.W., 2nd and T. Force, *Protein kinase cascades in the regulation of cardiac hypertrophy.* J Clin Invest, 2005. **115**(3): p. 527-37.

35. Ahn, M., et al., *Regulation of Na(v)1.2 channels by brain-derived neurotrophic factor, TrkB, and associated Fyn kinase.* J Neurosci, 2007. **27**(43): p. 11533-42.

36. Voss, M., et al., *Phospholipase D stimulation by receptor tyrosine kinases mediated by protein kinase C and a Ras/Ral signaling cascade.* J Biol Chem, 1999. **274**(49): p. 34691-8.

37. Nishio, H., et al., *Possible involvement of calcineurin, protein kinase C, and Src-family kinases in angiotensin II-induced tyrosine phosphorylation of p130cas in rat cardiac muscle.* Leg Med (Tokyo), 1999. **1**(2): p. 105-10.

38. Hsu, K.L., et al., *Protein kinase C-Fyn kinase cascade mediates the oleic acid-induced disassembly of neonatal rat cardiomyocyte adherens junctions.* Int J Biochem Cell Biol, 2009. **41**(7): p. 1536-46.

39. Strauss, O., S. Mergler, and M. Wiederholt, *Regulation of L-type calcium channels by protein tyrosine kinase and protein kinase C in cultured rat and human retinal pigment epithelial cells.* FASEB J, 1997. **11**(11): p. 859-67.

40. Chen, M.H., R. Kerkela, and T. Force, *Mechanisms of cardiac dysfunction associated with tyrosine kinase inhibitor cancer therapeutics.* Circulation, 2008. **118**(1): p. 84-95.

41. Atwood, B.K., et al., *Expression of G protein-coupled receptors and related proteins in HEK293, AtT20, BV2, and N18 cell lines as revealed by microarray analysis.* BMC Genomics, 2011. **12**: p. 14.

42. Martiny-Baron, G., et al., *Selective inhibition of protein kinase C isozymes by the indolocarbazole Go 6976.* J Biol Chem, 1993. **268**(13): p. 9194-7.

43. Goekjian, P.G. and M.R. Jirousek, *Protein kinase C in the treatment of disease: signal transduction pathways, inhibitors, and agents in development.* Curr Med Chem, 1999. **6**(9): p. 877-903.

44. Sakmann, B. and E. Neher, *Single-channel recording*. 2nd ed. 1995, New York: Plenum Press. xxii, 700 p.

45. Michael, A.C. and L.M. Borland, *Electrochemical methods for neuroscience*. Frontiers in neuroengineering series. 2007, Boca Raton: CRC Press. 512 p.

46. Wang, P. and Q. Liu, *Cell-based biosensors : principles and applications*. Artech House series engineering in medicine & biology. 2010, Boston: Artech House. xvii, 271 p.

47. ten Tusscher, K.H., et al., *A model for human ventricular tissue.* Am J Physiol Heart Circ Physiol, 2004. **286**(4): p. H1573-89.

48. Ten Tusscher, K.H. and A.V. Panfilov, *Cell model for efficient simulation of wave propagation in human ventricular tissue under normal and pathological conditions.* Phys Med Biol, 2006. **51**(23): p. 6141-56.

49. ten Tusscher, K.H. and A.V. Panfilov, *Alternans and spiral breakup in a human ventricular tissue model.* Am J Physiol Heart Circ Physiol, 2006. **291**(3): p. H1088-100.

50. Hund, T.J. and Y. Rudy, *Rate dependence and regulation of action potential and calcium transient in a canine cardiac ventricular cell model.* Circulation, 2004. **110**(20): p. 3168-74.

51. Zygmunt, A.C., et al., *Larger late sodium conductance in M cells contributes to electrical heterogeneity in canine ventricle.* Am J Physiol Heart Circ Physiol, 2001. **281**(2): p. H689-97.

52. Luo, C.H. and Y. Rudy, *A dynamic model of the cardiac ventricular action potential. I. Simulations of ionic currents and concentration changes.* Circ Res, 1994. **74**(6): p. 1071-96.

53. Terrenoire, C., et al., *Autonomic control of cardiac action potentials: role of potassium channel kinetics in response to sympathetic stimulation.* Circ Res, 2005. **96**(5): p. e25-34.

54. Nagatomo, T., et al., *Temperature dependence of early and late currents in human cardiac wild-type and long Q-T DeltaKPQ Na+ channels.* Am J Physiol, 1998. **275**(6 Pt 2): p. H2016-24.

55. Coste, B., et al., *Gating and modulation of presumptive NaV1.9 channels in enteric and spinal sensory neurons.* Mol Cell Neurosci, 2004. **26**(1): p. 123-34.

56. Vargas, G., et al., *Common components of patch-clamp internal recording solutions can significantly affect protein kinase A activity.* Brain Res, 1999. **828**(1-2): p. 169-73.

57. Ono, K. and M. Arita, *Mechanism of fluoride action on the L-type calcium channel in cardiac ventricular myocytes.* Cell Calcium, 1999. **26**(1-2): p. 37-47.

58. Chen, Y. and N.J. Penington, *Competition between internal AlF(4)(-) and receptor-mediated stimulation of dorsal raphe neuron G-proteins coupled to calcium current inhibition.* J Neurophysiol, 2000. **83**(3): p. 1273-82.

59. Wang, P., et al., *Mechanisms of sodium fluoride-induced endothelial cell barrier dysfunction: role of MLC phosphorylation.* Am J Physiol Lung Cell Mol Physiol, 2001. **281**(6): p. L1472-83.

60. Suwalsky, M., et al., *Aluminum fluoride affects the structure and functions of cell membranes.* Food Chem Toxicol, 2004. **42**(6): p. 925-33.

61. Cummins, T.R., et al., *Voltage-clamp and current-clamp recordings from mammalian DRG neurons.* Nat Protoc, 2009. **4**(8): p. 1103-12.

62. Malhotra, J.D., et al., *Tyrosine-phosphorylated and nonphosphorylated sodium channel beta1 subunits are differentially localized in cardiac myocytes.* J Biol Chem, 2004. **279**(39): p. 40748-54.

63. Ko, S.H., et al., *Modulation of Na(v)1.5 by beta1-- and beta3-subunit co-expression in mammalian cells.* Pflugers Arch, 2005. **449**(4): p. 403-12.

64. Moran, O., M. Nizzari, and F. Conti, *Endogenous expression of the beta1A sodium channel subunit in HEK-293 cells.* FEBS Lett, 2000. **473**(2): p. 132-4.

65. Jiang, X., et al., *Modulation of CaV2.1 channels by Ca2+/calmodulin-dependent protein kinase II bound to the C-terminal domain.* Proc Natl Acad Sci U S A, 2008. **105**(1): p. 341-6.

66. Wagner, S., et al., *Ca2+/calmodulin-dependent protein kinase II regulates cardiac Na+ channels.* J Clin Invest, 2006. **116**(12): p. 3127-38.

67. Yoon, J.Y., et al., *Constitutive CaMKII activity regulates Na+ channel in rat ventricular myocytes.* J Mol Cell Cardiol, 2009. **47**(4): p. 475-84.

68. Missan, S., P. Linsdell, and T.F. McDonald, *Tyrosine kinase and phosphatase regulation of slow delayed-rectifier K+ current in guinea-pig ventricular myocytes.* J Physiol, 2006. **573**(Pt 2): p. 469-82.

69. Okubo, S., et al., *Tyrosine kinase signaling in action potential shortening and expression of HSP72 in late preconditioning.* Am J Physiol Heart Circ Physiol, 2000. **279**(5): p. H2269-76.

70. Sobko, A., A. Peretz, and B. Attali, *Constitutive activation of delayed-rectifier potassium channels by a src family tyrosine kinase in Schwann cells.* EMBO J, 1998. **17**(16): p. 4723-34.

71. Aydin, O., et al., *Effects of protein kinase C activation on cardiac repolarization and arrhythmogenesis in Langendorff-perfused rabbit hearts.* Europace, 2007. **9**(11): p. 1094-8.

72. McHugh, D., et al., *Inhibition of cardiac L-type calcium channels by protein kinase C phosphorylation of two sites in the N-terminal domain.* Proc Natl Acad Sci U S A, 2000. **97**(22): p. 12334-8.

73. Gershome, C., et al., *Colocalization of voltage-gated Na+ channels with the Na+/Ca2+ exchanger in rabbit cardiomyocytes during development.* Am J Physiol Heart Circ Physiol, 2011. **300**(1): p. H300-11.

74. Numann, R., et al., *Modulation of skeletal muscle sodium channels in a satellite cell line by protein kinase C.* J Neurosci, 1994. **14**(7): p. 4226-36.

75. Bendahhou, S., et al., *Serine-1321-independent regulation of the mu 1 adult skeletal muscle Na+ channel by protein kinase C.* Proc Natl Acad Sci U S A, 1995. **92**(26): p. 12003-7.

76. Strauss, O., et al., *Effects of protein kinase C on delayed rectifier K+ channel regulation by tyrosine kinase in rat retinal pigment epithelial cells.* Invest Ophthalmol Vis Sci, 2002. **43**(5): p. 1645-54.

77. Copel, C., et al., *Activation of neurokinin 3 receptor increases Na(v)1.9 current in enteric neurons.* J Physiol, 2009. **587**(Pt 7): p. 1461-79.

78. Clark, J.W., et al., *EMBS-BMES 2002 : Second Joint EMBS/BMES Conference : conference proceedings : Bioengineering--integrative methodologies, new technologies : 23-26 October, Houston, Texas, USA*. 2002, Piscataway, New Jersey: IEEE.

79. Wang, Y., et al., *Inhibition of fast sodium current in rabbit ventricular myocytes by protein tyrosine kinase inhibitors.* Pflugers Arch, 2003. **446**(4): p. 485-91.

80. Katare, R.G., et al., *Novel bisindolylmaleimide derivative inhibits mitochondrial permeability transition pore and protects the heart from reperfusion injury.* Can J Physiol Pharmacol, 2007. **85**(10): p. 979-85.

81. Edwards, A.S., et al., *Carboxyl-terminal phosphorylation regulates the function and subcellular localization of protein kinase C betaII.* J Biol Chem, 1999. **274**(10): p. 6461-8.

82. Sieg, D.J., et al., *Pyk2 and Src-family protein-tyrosine kinases compensate for the loss of FAK in fibronectin-stimulated signaling events but Pyk2 does not fully function to enhance FAK- cell migration.* EMBO J, 1998. **17**(20): p. 5933-47.

83. Ferdinandy, P., R. Schulz, and G.F. Baxter, *Interaction of cardiovascular risk factors with myocardial ischemia/reperfusion injury, preconditioning, and postconditioning.* Pharmacol Rev, 2007. **59**(4): p. 418-58.

84. Dawn, B., et al., *Bifunctional role of protein tyrosine kinases in late preconditioning against myocardial stunning in conscious rabbits.* Circ Res, 1999. **85**(12): p. 1154-63.

85. Yamada, E., et al., *Fyn-dependent regulation of energy expenditure and body weight is mediated by tyrosine phosphorylation of LKB1.* Cell Metab, 2010. **11**(2): p. 113-24.

86. Blake, R.A., et al., *SU6656, a selective src family kinase inhibitor, used to probe growth factor signaling.* Mol Cell Biol, 2000. **20**(23): p. 9018-27.

87. Haouala, A., et al., *Drug interactions with the tyrosine kinase inhibitors imatinib, dasatinib, and nilotinib.* Blood, 2011. **117**(8): p. e75-87.

88. Lin, Y.C., et al., *Rescue of a trafficking defective human pacemaker channel via a novel mechanism: roles of Src, Fyn, and Yes tyrosine kinases.* J Biol Chem, 2009. **284**(44): p. 30433-40.